

5. FORMULATION & DEVELOPMENT OF HNCs

5.1 INTRODUCTION

Novel, integrated systems known as Hybrid nanocarriers (HNCs) have been introduced in an effort to mitigate some limitations associated with liposomes and PNPs (1). Briefly, the biomimetic characteristics of lipids and architectural advantage of polymer core are combined to yield a theoretically superior delivery system. HNCs are solid, submicron particles composed of at least two components: the polymer and the lipid. Various bioactive molecules such as drugs, genes, proteins, and targeting ligands can be entrapped, adsorbed, or covalently attached in the hybrid system. The common choices of biodegradable polymers include polylactic-co-glycolic acid (PLGA), Polycaprolactone (PCL), dextran, PEG-PLA, PEG-PCL or albumin because of their biocompatibility, biodegradability, nontoxicity, and previous use in approved products (2, 3). Lipids used are often zwitterionic, cationic, anionic, and neutral phospholipids such as lecithin, 1,2-dipalmitoyl-sn-glycero-3-phosphocholine (DPPC), 1,2-dipalmitoyl-3-trimethylammonium-propane (DPTAP), 1,2-dioleoyl-3-trimethylammonium-propane (DOTAP), or 1,2-dioleoyl-sn-glycero-3-phosphoethanolamine (DOPE) (4-8).

5.2 EXPERIMENTAL WORK

5.2.1 Materials

Table 5-1 List of materials used with their sources

Sr no.	Material Category	Name	Supplier of Material
1	Drug	Cisplatin	Gift sample from Sun Pharmaceuticals Advanced Research Center (SPARC)
2	Polymer	PLGA(50:50)	Gift Sample from PURAC England
		PEG-PLA	
3	Phospholipids	Phospholipoin 90G (Soy Phosphatidylcholine)	Gift samples from Lipoid, Germany
		1,2-dipalmitoyl-sn-glycero-3-phosphocholine (DPPC)	
		Cholesterol	
		Didioleoyltrimethylammoniumpropane (DOTAP)	
		Dioleoyl phosphatidyl ethanolamine (DOPE)	
		1,2-distearoyl-sn-glycero-3-phosphoethanolamine-N-[carboxy(polyethylene glycol)-2000] (sodium salt) (DSPE-PEG)	
4	Surfactants	Poly Vinyl Alcohol(PVA) cold water soluble	Hi-media, India
		Poloxamer 407	Sigma Aldrich , USA
		Tween 80	
5	Solvents	Acetone (Analytical Grade)	S D Fine Chemicals, India
		Chloroform(Analytical Grade)	
		Potassium Dihydrogen Phosphate	
		Sodium hydroxide Pellets	
		Glacial Acetic acid	
		Hydrochloric Acid	S.D. Fine Chemicals
		Sodium Acetate Trihydrate	Lipoid GmbH, Germany.
		Acetonitrile (Analytical grade)	Astron
		Acetonitrile (HPLC grade)	Astron

5.2.2 Instruments

Table 5-2 List of Equipment Used

Sr. No.	Equipment	Company
1.	Single pan electronic balance	Type AX 120 & ELB 300, Shimadzu
2.	UV Visible Spectrophotometer	UV-1800, Pharm Spec, Shimadzu, Japan
3.	HPLC	Agilent Technologies 1260 infinity II
4.	Bath sonicator	Sartorius, India
5.	Rotary evaporator	IKA Rotavapor RV-10, IKA® India Private Limited
6.	Magnetic stirrer	Remi, India
7.	Virtis Advantage Plus Lyophilizer	Virtis
8.	Centrifuge (CPR-30)	Remi Elektrotechnik Ltd., Vasai, India
9.	Dialysis Membrane-70 (pore size 7000 daltons, Diameter 27.3 mm)	Himedia Laboratories Pvt. Ltd. Mumbai.
10	Extruder	Avestin, USA

5.3 METHODS

5.3.1 Preliminary optimization and screening

HNCs are the amalgamation of properties of liposomes and Nanoparticles providing advantageous size range (10-200 nm) favourable for endocytotic intercellular uptake, accumulation in the tumor site through leaky tumor vascular structures, which is useful for prolonged drug exposure to the tumor site and good structural stability (9, 10). HNCs can be synthesized through two distinct approaches. One approach involves a two-step process in which the polymer core and lipid shell are prepared separately and then added and mixed together; the other approach involves a single-step process, in which the hybrid nanoparticles are prepared through a single step nanoprecipitation and self-assembly method. It was observed that two step method of preparation provided encapsulation efficiency of cisplatin below 40 % which may be due to leaching of the drug during incubation step due to its water-soluble nature. Further, evaluation of the formulation also revealed existence of liposomes and polymeric core as distinct phases in cryo-TEM images instead of polymeric core covered by a layer of lipid, which was the target attribute for the formulation. It was also noted that the method is complex, time consuming and less efficient due to preparation of polymeric core and liposomes separately. One step approach like lipo-polymeric film formation followed by hydration can also be used

HNCs formulation

to formulate HNCs and drug loading is generally expected to be better in the incorporation approach than the two step/adsorption approach (11-13). One reason for poor drug loading (DL) and entrapment efficiency (EE) in HNCs is the presence of excess lipids that can form vesicles by entrapment or adsorption of drug via hydrophobic interactions and/or hydrogen bonding which during purification, these vesicles are washed away, leading to drug loss. Therefore, the amount of the lipid required to uniformly coat the core nanoparticles has to be optimized using empirical and/or experimental techniques. All the methods listed in Chapter 1 were checked for their feasibility and the best method suited to Cisplatin caprylate HNCs with favorable characteristics was further optimized.

5.3.2 One step method using Thin lipo-polymeric film formation followed by hydration and extrusion:

5.3.2.1 Optimization of process parameters

Different process parameters involved in the preparation of HNCs were optimized initially. These process parameters included solvent evaporation time, hydration time and rotation speed of RBF during hydration were optimized for desired results. While keeping other factors constant, effect of one variable was observed on desired output parameters. The process parameters were evaluated and optimized based on formulation containing key excipients like DPPC, DOPE, PEG-PLA, PLGA etc.

5.4 QUALITY BY DESIGN & DESIGN OF EXPERIMENT (QBD-DOE) APPROACH FOR HNCs FORMULATION AND OPTIMIZATION

Optimization by changing one variable at a time is a complex procedure to evaluate the effects of different variables on an experimental outcome. This approach is time consuming and sometimes leads to misinterpretation of results. Another approach known as Response Surface Methodology is used to accurately evaluate the impact of independent variables on the dependent variables by varying all the important factor simultaneously in systemic manner. In this approach, BBD was used for optimization of parameters for following reasons:

- It requires less runs than 3-factor, 3-level Full Factorial Design and Central Composite Design (CCD) when at least three factors are included.

HNCs formulation

- BBD is a spherical design with excellent predictability within the spherical design space. Compared with the CCD method, the BBD technique is considered as the most suitable for evaluating quadratic response surfaces particularly in cases when prediction of response at the extreme level is not the goal of the model.
- This cubic structure is described by a lot of focuses lying at the midpoint of each edge and a repeat focus purpose of the multidimensional 3D cubic shape.

Box-Behnken design matrix was generated using Design Expert 7.0 software which gave 15 experimental run. Lipid concentration (mM), polymer concentration (mg/ml) and lipid molar ratio were selected as independent variables. Nanocarrier size (nm) and % entrapment efficiency of cisplatin caprylate in HNCs were taken as dependent (response) variables. Design Expert 7.0.0 was used to generate Box-Behnken design.

5.4.1 Procedure for formulation of HNCs

Hybrid nanocarriers were formulated using thin film formation followed by hydration and extrusion (11). Primary lipid (DPPC), secondary lipids (Cholesterol, DOPE, DOTAP), and polymer (PEG-PLA) were dissolved in required ratio and concentration as per BBD batches in solvent chloroform in a flask. The lipo-polymeric film was formed by evaporation of organic solvent using flow of nitrogen gas. The film was then further dried in a vacuum desiccator overnight at 100 mmHg & 25°C to remove residual solvent. The film was hydrated using phosphate buffered saline (PBS) pH 7.4 containing cisplatin caprylate (1 mg/mL) at 45°C for 15 min in water bath and subsequently bath sonicated at 45°C for complete hydration. The hydrated vesicles were subsequently extruded five times by Genizer high pressure extruder through 200 nm polycarbonate membranes (polyethylene drain disk was used to support polycarbonate membrane to potentiate extrusion process) to obtain monodisperse & uni-lamellar HNCs. Post insertion technique was used to incorporate DSPE-PEG 2000 and/or DSPE-PEG 2000 folate (3 mol% of total lipid contents) into preformulated HNCs aqueous dispersion as per PEGylation and targeting requirement. For this, DSPE-PEG 2000 was mixed below critical micellar concentration (CMC) level (10 µM) to HNCs aqueous dispersion in water bath at glass

transition temperature T_g (42°C) under gentle agitation for 30min to obtain PEGylated counterparts (7, 12).

Characterization of Cisplatin caprylate loaded HNCs

5.4.2 Dynamic light scattering (DLS) Nanocarrier size analysis

Size of HNCs was determined using principle of dynamic light scattering using Malvern Zetasizer Nano (Nano ZS, Malvern Instruments, UK). Light source was 633 nm He-Ne laser and scattering angle was 175°. Analyses were carried out at 25°C temperature after diluting 0.2 ml of formulation to 2 ml using filtered double distilled water. The total number of sub-runs for measurement of size were 15 and each run was for a duration of 10 seconds. The results were reported as Z-average along with polydispersity index after carrying out analysis in triplicate. A homogenous sample is represented by a PDI close to 0.00 while a highly polydisperse sample has a PDI close to 1.00.

5.4.3 Zeta potential analysis

Zeta potential values were obtained using Smoluchowski equation which takes into account electrophoretic mobility of the particles and 175° back-scatter. A 0.2 ml of volume of liposomes were diluted up to 2 ml with double distilled water and analysis was carried out in triplicate using zeta cuvette at 25°C. The measurements were done using ZetaSizerNanoZS (Malvern Instruments Ltd., UK) in triplicate.

5.4.4 Entrapment efficiency and drug loading

Centrifugation method was used for separation of free drug from HNCs. For this 1 mL of HNCs dispersion was taken in a 1.5 mL micro-centrifuge tube. The tubes were centrifuged at 15000 RPM for 30 mins & 10 C to settle down the free cisplatin, cisplatin caprylate and excess lipid and polymer at the bottom of the centrifuge tube. The Supernatant containing HNCs are collected in separate vial. The entrapped drug was determined by analyzing supernatant after centrifugation. The 1 ml of supernatant sample was taken in a 10 mL volumetric flask and was diluted with Methanol: Acetonitrile (1:2) to make 10ml and the entrapped drug amount in 1 mL formulation was determined by derivatization method through colorimetry at 705 nm. The entrapment efficiency was calculated by following equation:

$$\text{Entrapment efficiency} = \frac{\text{Entrapped drug}}{\text{Total drug}} * 100$$

Drug loading

For determination of loading efficiency of HNCs, following equation was used:

$$\% \text{ Drug Loading Efficiency} = \frac{\text{amount of Cisplatin in HNCs}}{\text{total solid content (Cisplatin + excipients)}} * 100$$

5.4.5 Transmission Electron Microscopy (TEM)

TEM experiments were carried out on a Technai, Phillips Holland, at Sophisticated Instrumentation Center for applied Research and testing (SICART), Vallabh Vidyanagar instrument at an acceleration voltage of 200 kV. The TEM sample was prepared by administering the HNCs onto a 300-mesh Formvar-coated copper grid that had been previously hydrophilized under UV light (Electron Microscopy Sciences, Hatfield, PA). Samples were blotted away after 30 min incubation and grids were negatively stained for 10 min at room temperature with freshly prepared and sterile-filtered 2% (w/v) uranyl acetate aqueous solution. The grids were then washed twice with distilled water and air dried prior to imaging (14).

Morphology and size of HNCs were also evaluated using Cryo Transmission Electron Microscopy (TECNAI G2 Spirit BioT WIN, FEI-Netherlands) operating at 200 kV with 0.27 nm resolution. The hydrophobic grid was converted into hydrophilic by glow discharge. The samples were spread on grid and cryo-frozen in liquid ethane at -180°C. The grid was inserted into microscope using a cryo holder and images were taken at 70,000X magnification. Cryo-TEM experiments were carried out at CSMCRI, CSIR institute, Bhavnagar.

5.4.6 Scanning Electron Microscopy (SEM) Analysis

For determination of particle morphology SEM was performed using EVO-18 ZEISS, at Metallurgy Department, Maharaja Sayajirao Rao University of Baroda. SEM analysis was done for HNCs by drying the HNCs dispersion on grid and viewing immediately.

5.4.7 *In-vitro* drug release study and drug release kinetic

The *In-vitro* drug release from Cisplatin caprylate loaded HNCs were evaluated at three different pH values, pH 5.5, pH 6.6 and pH 7.4. This was done in order to imitate three physiological conditions that exist in a cancer patient, the pH of

HNCs formulation

the blood and normal tissue is 7.4, the pH at the cancer tissue is 6.6 and the pH inside the cancer cells range from 5-6. Dialysis bag (cellulose membrane 12 KDa; HiMedia) set up was used for *in-vitro* drug release study of Cisplatin caprylate. A 5 cm long piece of activated dialysis bag was tied up tightly at one end with nylon thread taking care that no leakage of content from the sac would occur from the tied portion. The optimized batches of Cisplatin caprylate HNCs and then filled in the dialysis sac. The dialysis sac was tied up at the second end firmly making sure that no leakage occurs from this end also. This sac would act as a donor compartment. 100 mL phosphate buffer of pH 7.4 was taken in a beaker and the filled dialysis sac was suspended in the buffer. The buffer was maintained at 37°C temperature and being constantly stirred with Teflon coated bar magnet on a magnetic stirrer with heating plate. The beaker was kept closed with aluminium foil to prevent any loss of volume due to evaporation. 1 mL samples of dialysis buffer in receptor compartment were sampled from the beaker into 1.5 mL Eppendorf tubes at regular time intervals for up to 96 hr and analyzed for Cisplatin caprylate content. Immediately after each sampling, the dialysing buffer was replenished with 1 mL of fresh buffer. Cisplatin caprylate released in dialysis buffer was determined by derivatization method of ligand exchange reaction between cisplatin caprylate and orthophenylenediamine (OPDA) and resulting green color adduct can be detected by colorimetry at 705 nm. The absorbance was recorded for the solution and amount and percentage of Cisplatin caprylate released was determined. Drug release data are fitted in zero order, first order, Higuchi, Korsmeyer–Peppas and Hixon-crowell models to determine release kinetic pattern from HNCs (10, 15).

1. Zero order release

Following equation can be applied for drug release that follows zero order kinetics.

$$M_t = kt$$

Where, M_t = amount of drug released at time t

k = zero order release rate constant

t = time

2. First order release

Following equation can be applied for drug release that follows first order kinetics.

$$\ln[1-(M_t/M_0)] = -kt$$

Where, M_t = amount of drug released at time t

M_0 = initial amount of drug present

k = first order release rate constant

t = time

3. Higuchi's model

Following equation can be applied for drug release that follows Higuchi's kinetics model.

$$M_t = kt^{1/2}$$

Where, M_t = amount of drug release at time t

k = Higuchi's release rate constant

t = time

4. Korsmeyer –Peppas model

Following equation can be applied for drug release that follows Korsmeyer –Peppas kinetics model.

$$\ln M_t/M_0 = \ln k + n \ln t$$

Where, M_t = amount of drug released at time t

M_0 = initial amount of drug present

k = Korsmeyer –Peppas release rate constant

t = time

n = Diffusional exponent that characterizes the mechanism of drug release.

The value of diffusional exponent 'n' will help to understand mechanism of drug release from dosage forms of different geometry like slab, cylinder, sphere etc.

- $n = 0.5$ to 1 ($0.5 < n < 1$) indicates non Fickian release
- $n = 0.5$ indicates Higuchi's Kinetics
- $n = 1$ indicates the first order release or case 2 transport.
- $n < 0.5$ indicates Fickian release.
- $n > 1$ indicates the Super case 2 transport.

5. Hixon Crowell model

Following equation can be applied for drug release that follows Hixon Crowell kinetics model.

$$\sqrt[3]{M_0} - \sqrt[3]{M_t} = kt$$

Where, M_t = amount of drug released at time t

M_0 = initial amount of drug present

k = Hixon Crowell release rate constant; t = time

Solutions:

- **Sodium Sulphide solution 0.3%:** 0.3 g of accurately weighed sodium sulphide was dissolved in sufficient quantity of distilled water to produce 100 mL.
- **Sulphuric acid solution 0.2%:** 0.2 mL of concentrated sulphuric acid was dissolved in sufficient quantity of distilled water to produce 100 mL.
- **Potassium Dihydrogen Phosphate, 0.2M (17):** 27.218 g of potassium dihydrogen phosphate was dissolved in sufficient quantity of distilled water to produce 1000 mL.
- **Sodium Hydroxide, 0.2M (17):** 8.0 g of sodium hydroxide was dissolved in sufficient quantity of distilled water to produce 1000 mL.
- **Phosphate Buffer(17):** 50.0 mL of the 0.2M potassium dihydrogen phosphate, 0.2M was taken in a 200-mL volumetric flask and specified volume of 0.2M sodium hydroxide, 0.2M and then water was added to make the final volume. The pH of the buffer was checked using pH meter and adjusted if needed using sodium hydroxide solution or hydrochloric acid solution as necessary.

Amount of 0.2M NaOH to be added to 0.2M KH_2PO_4 Solution to get Buffer of Required pH

pH	0.2 M NaOH (mL)
6.6	16.4
7.4	39.1

- **Acetic acid solution 2N(18)** 116 mL of glacial acetic acid was dissolved in sufficient quantity of distilled water and after cooling of solution to room temperature final volume was made to 1000 mL.
- **Acetate Buffer pH 5.5 (18):** 5.98 g of sodium acetate trihydrate was weighed and sampled in a 1000 mL volumetric flask. To this 3.0 mL of the acetic acid solution was added and volume was made up to 1000 mL. The pH of the

HNCs formulation

buffer was checked using pH meter and adjusted if needed using acetic acid solution or sodium hydroxide solution as necessary.

Dialysis membrane Set-Up/activation

Before using the dialysis membrane for drug release study it was first activated by following process.

1. 5cm long dialysis membrane was cut and was kept in running water for 3 hr for the removal of glycerin.
2. After 3 hrs dialysis membrane was dipped in 0.3% w/v solution of Sodium sulphide solution at 80°C for 1 min.
3. Sodium sulphide treated Dialysis membrane was then dipped in warm water at 60°C for 1 min to remove sodium sulphide.
4. Dialysis membrane was then dipped in 0.2 % H₂SO₄ for 1 min.
5. Then it was again dipped in the warm water for removal of H₂SO₄.

This activated dialysis membrane was then kept in Phosphate buffer (pH 7.4) for 24 hr prior to drug release studies.

5.4.8 Phospholipid content by Stewart method

Total Phospholipid content was measured in the formulation. 2ml formulation was taken and same procedure was done as per show in chapter 3.

5.4.9 Estimation of residual solvent by HS-Gas Chromatography

Standard Preparation: Standard sample for Chloroform was done by taking 100µl chloroform in 10ml volumetric flask and make upto the mark using DMF so the concentration will be 10.000 ppm. From the above solution, take 1ml in 10ml volumetric flask and make upto the mark using Deionized water, so the concentration will be 1000 ppm.

Sample Preparation: 100µl formulation was taken in 10ml volumetric flask and make upto the mark with DMF. From the above solution, take 1ml in 5ml volumetric flask and make up the volume by using Deionized water (16).

5.4.10 Small angle X Ray scattering (SAXS)

SAXS measurement was carried out with Anton Par SAXspace at IMTech, Chandigarh in line collimation having wavelength of 0.154 nm in Thermostated Quartz Capillary with 1mm thickness at 25 C. Beam exposure time was 15 mins and diffraction patterns were checked and set in accordance with beam decay with

background subtractions and detector alignment. The X-ray path length through the sample was 1 mm. Scattering intensities were plotted as a function of the scattering vector against wavelength. Results were analyzed by ATSAS2.8.3 software and inter atomic distribution was checked by In-built AUTOGNOM in the SAXS instrument.

5.5 RESULTS AND DISCUSSION

5.5.1 Optimization of process parameters

Process parameters like solvent, solvent evaporation temperature & time, vacuum condition, rotation speed, extrusion cycles etc. were optimized as per following:

Table 5-3 Effect of process parameters for formation of films

Solvent	Observation
Chloroform	Suitable as all lipids, polymer and drug are soluble in chloroform.
Solvent evaporation temperature	
Temperature (°C)	Observation
45°C	Suitable for evaporation of solvent under reduced pressure based on the Tg of the lipids
Solvent evaporation time (at 48°C, 100 rpm, 400 mmHg)	
Time (min)	Observation
30	Efficient drying
60	Efficient drying
90	No further improvement
Vacuum condition (30 minute at 48°C and 100 rpm)	
Vacuum (mmHg)	Observation
200	Inefficient drying
300	Inefficient drying
400	Thin uniform film
450	Thin uniform film
Rotation speed (for 30 minutes at 48°C and 450 mmHg)	
Rotation speed (rpm)	Observation
50	Localized deposits on the wall with uneven film thickness
80	Thin uniform film
100	Thin uniform film
120	Uniform to noncontiguous films with gaps in between
150	Noncontiguous films with gaps in between
Extrusion cycles	
Cycles	Size(nm)
No cycle	382
3 cycles	187

5 Cycles	181
7 Cycles	176
All experiments were performed in triplicate.	

5.5.2 Preliminary screening of formulation components

Table 5.4 shows the size distribution, zeta potential, entrapment efficiency and drug loading of drug loaded liposomes as well as various batches of drug loaded non-PEGylated and PEGylated HNCs. V1 to V3 batches were non-PEGylated ones that were preliminarily screened to evaluate effect of addition of copolymer and cationic lipid to the lipid composition. All these batches exhibited size in the range of 120-140 nm. The entrapment efficiency of cisplatin caprylate in liposomes of batch V1 was found to be 35.3% only which might be due to loading only in bilayer compartment of liposomes. Batch V2 and V3 were prepared with block co-polymeric component along with the lipid components and exhibited improved entrapment efficiency of 65.6% and 68.5% respectively. The increment in drug loading from 3.20 mg to 4.21 mg was also observed due to incorporation of copolymer in the composition whose amphiphilic property would lead to partitioning of the drug in the core over and above that in lipid bilayer. One thing to note is that these batches were prepared without addition of cholesterol hence the overall fluidity of membrane would be less to tolerate the shear during processing leading to lesser drug entrapment as opposed to our previous findings as well as were prepared using film hydration technique instead of emulsion solvent evaporation method leading to comparatively lower entrapment values (10). Evaluation of the sedimented pellet after centrifugation confirmed these speculations. Effect of variation in lipid to polymer (L/P) weight ratio was evaluated by changes in size and entrapment of the formed HNCs in batches V4 to V7. Batch V4 showed 153.8 nm size with marginal increment which may be due to post insertion of the PEGylation layer, however had similar entrapment efficiency levels of cisplatin caprylate as that of batch V3. Herein, addition of cholesterol in the lipid composition improved the entrapment as well as loading. Conversely, reducing the L/P ratio along with increasing the cholesterol content (Batch V5) deteriorate the quality of HNCs. This observation substantiates the importance of lipid composition during PEGylation impacting packing characteristics and thus PDI (11). It was observed that the size of HNCs was significantly increased above 200 nm along with high polydispersity index when L/P weight ratio was kept higher (4:1, Batch V6) with increase in lipid

HNCs formulation

concentration to 10 mM. Furthermore, if L/P ratio was low (1:3 % w/w, Batch V7), higher PDI value was obtained indicating unfavourable balance of hydrophilic and hydrophobic groups between lipids and polymers which may lead to aggregate formation due to insufficient lipid coating. Zeta potential value was found to be decreased (~12mV) in such cases with lower L/P ratio. There was decrease in entrapment of cisplatin caprylate in batches V5 and V7 which indicated effect of L/P ratio on drug entrapment efficiency and drug loading. As polymer weight ratio increases, drug entrapment was found to decrease which may be due to insufficient lipid coating which also presents space for drug in the bilayer compartment (13). The finalized composition for further evaluation was batch V4.

Table 5-4 HNCs formulation Preliminary screening

Batch No	Formulation	Size (nm)	PDI	Zeta potential (mV)	Drug entrapment (%)	Drug loading g* (%)
V1	DPPC:DOPE:DOTA P - 6:2:2 (5 mM)	121.6±1.5	0.18±0.03	42.81±1.59	35.3±3.5	0.07
V2	DPPC:DOPE - 3:1 (5 mM), PEG-PLA (5mg/mL) & L:P - 3:1 w/w	134.3±1.9	0.15±0.03	22.47±0.89	65.5±4.9	3.20
V3	DPPC:DOPE:DOTA P - 6:2:2 (5 mM), PEG-PLA & L:P - 3:1 w/w	128.9±1.4	0.14±0.02	42.91±1.67	68.2±3.8	4.21
V4	DPPC:Cholesterol:DOPE:DOTAP-6:2:1:1 (5 mM), PEG-PLA (5mg/ml) & L:P - 3:1 w/w	153.8±1.6	0.15±0.03	38.16±0.79	84.9±2.2	7.29
V5	DPPC:Cholesterol:DOPE:DOTAP-4:4:1:1 (5 mM), PEG-PLA (5mg/ml) & L:P - 1:1 w/w	141.4±2.8	0.47±0.06	18.52±1.75	55.7±3.8	3.05
V6	DPPC:Cholesterol:DOPE:DOTAP-6:2:1:1 (10 mM), PEG-PLA (5mg/ml) & L:P - 4:1 w/w	200.1±5.5	0.48±0.08	35.63±0.59	40.9±2.6	6.26

HNCs formulation

Batch No	Formulation	Size (nm)	PDI	Zeta potential (mV)	Drug content (%)	Drug loading g* (%)
V7	DPPC:Cholesterol:D OPE:DOTAP-4:1:1:1 (5 mM), PEG-PLA (5mg/ml) & L:P - 1:3 w/w	148.7±3.2	0.53±0.05	12.58±0.78	42.5±2.9	5.20

PEG-PLA @ 5mg/mL; L:P- Lipid to Polymer ratio (w/w). *average values are reported. # Post insertion technique was used to incorporate DSPE-PEG 2000 (3 mol % of total lipid contents) in V4 to V7. All experiments were performed in triplicate.

5.5.3 Quality by design - design of experiment (QbD-DoE) approach for HNCs formulation and optimization

Following process parameters mentioned in Table 5-5 Selected variables for BBD were kept constant based upon results obtained in Table 5-4 and ranges (levels) of formulation variables were decided by considering results obtained on preliminary screening batches. The architecture of HNCs depends on lipid and polymer balance therefore both were selected as independent variables in addition to lipid molar ratio. All the lipids were prepared and stored as 100 mM stock solutions and they were diluted during formulation according to its concentration and quantity into HNCs.

Table 5-5 Selected variables for BBD

Sr. No.	Variables	Range
Formulation Variables		
1	Lipid Concentration (mM)	1.0 – 5.0
2	Polymer Concentration (mg/ml)	0.5 – 0.83
3	Lipid molar ratio	1.5 – 4.0
Variables to be kept constant (Process parameters)		
4	Solvent evaporation temperature (°C)	48
5	Solvent evaporation time (mins)	30
6	Vacuum condition (mm-Hg)	400
7	Rotation speed (rpm)	100
8	Extrusion cycles (Cycles)	3

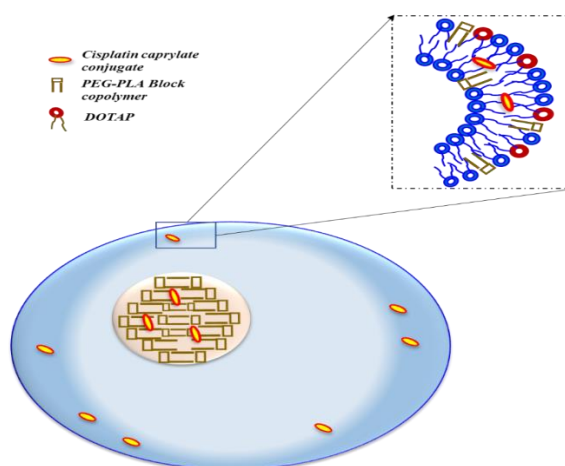


Figure 5-1 Schematic diagram of architecture of HNCs

HNCs were formulated by film hydration method followed by extrusion. Schematic structure of HNCs is shown in Figure 5-1. After thin lipo-polymeric film formation, self-assembly phenomenon occurs upon film hydration with phosphate buffer saline pH 7.4. Lipids and di-block co-polymer self-assemble themselves to align according to hydrophobic interaction to decrease surface free energy of hybrid system. The unique architecture of these hybrid nanocarriers is formation of polymeric solid matrix core inside lipid bilayer. Hydrophobic drug or hydrophilic drug can be encapsulated by PEG-PLA polymer which forms solid matrix core inside HNCs. The key attribute of this HNCs system is formation of hydrophobic core inside internal aqueous cavity of hybrid system and they are stabilized by forces like van der Waals forces, electrostatic interactions and hydrophobic attractions. Hydrating the film above glass transition temperature of lipid mixtures and sonication also assist in self-assembly process of hybrid nanocarrier formation. DPPC (glass transition temperature 41 C) was a primary lipid to form hybrid nanocarriers and it also assist to release its cargo in cancerous tissues having temperature (39-40 C) higher than normal body temperature. pH sensitive characteristics is due to the DOPE which helps nanocarriers for endosomal escape. Fatty acid carboxyl ions of DOPE makes nanocarrier stable at lamellar phase in neutral pH due to electrostatic repulsion but at acidic pH, these groups are protonated, converting them into the unstable hexagonal phase which in turn fuse, aggregate and release the cargo into the cytosol easily. Furthermore,

HNCs formulation

DOTAP was added to impart cationic charge to nanocarriers for effective complexation of negatively charged siRNA.

Box-behnken design matrix generated design batches as per given in table 5.7 according to independent & dependent variables given in table 5.6. The results of design batches are depicted as dependent variables as given in table 5.7.

Table 5-6 Variables and levels selected for preliminary study

Independent variables	Levels		
	-1	0	+1
A Lipid Concentration (mM)	1.0	3.0	5.0
B Polymer Concentration (mg/ml)	0.50	0.67	0.83
C Lipid molar ratio (DPPC:Chol)	1.50	2.75	4.00
Dependent variables			
Y1 Particle size (nm)			
Y2 % Entrapment efficiency (%)			

Table 5-7 Optimization of formulation parameter using BBD

Run	Independent variables			Dependent variables		
	Lipid Concentration	Polymer Concentration (mg/ml)	Lipid molar ratio #	Nanoparticles Size (nm)	Entrapment efficiency (%)	Drug loading (%)
F1	5.00	0.67	1.50	194.2±1.86	68.18±3.21	7.25
F2	1.00	0.50	2.75	142.1±2.69	41.92±2.67	3.77
F3	3.00	0.67	2.75	156.5±4.21	63.61±1.69	6.12
F4	1.00	0.67	4.00	136.2±1.84	46.82±2.80	3.94
F5	3.00	0.83	1.50	164.6±2.39	62.43±1.83	6.08
F6	3.00	0.83	4.00	144.7±3.26	64.36±2.78	6.18
F7	5.00	0.50	2.75	174.1±1.84	67.53±2.56	6.24
F8	3.00	0.50	1.50	169.5±2.63	56.12±1.89	5.12
F9	1.00	0.83	2.75	136.9±1.69	53.11±3.21	4.68
F10	1.00	0.67	1.50	144.7±1.27	41.39±2.69	3.78
F11	5.00	0.67	4.00	169.2±3.84	70.21±2.93	7.26
F12	3.00	0.50	4.00	149.3±2.78	58.05±1.11	5.20
F13	3.00	0.67	2.75	157.9±3.21	60.98±3.83	5.81
F14	3.00	0.67	2.75	151.5±1.27	61.66±2.17	5.86
F15	5.00	0.83	2.75	173.7±2.38	76.97±1.48	8.29

#Lipid molar ratio- It is ratio of DPPC and Cholesterol (DPPC:Cholesterol-3:2=1.50) where DOPE and DOTAP were kept constant in all formulations e.g. F1: DPPC:cholesterol:DOPE:DOTAP-3:2:1:1 at 5 mM total lipid concentration. *Drug loading- average values are reported. All experiments were performed in triplicate.

Nanocarrier size distribution was measured using Malvern Nano ZS for all design batches F1 to F15 are depicted in Figure 2A to 2I.

(Figure 5-2 Intensity based Nanocarrier size distribution: batch F1 to F15)

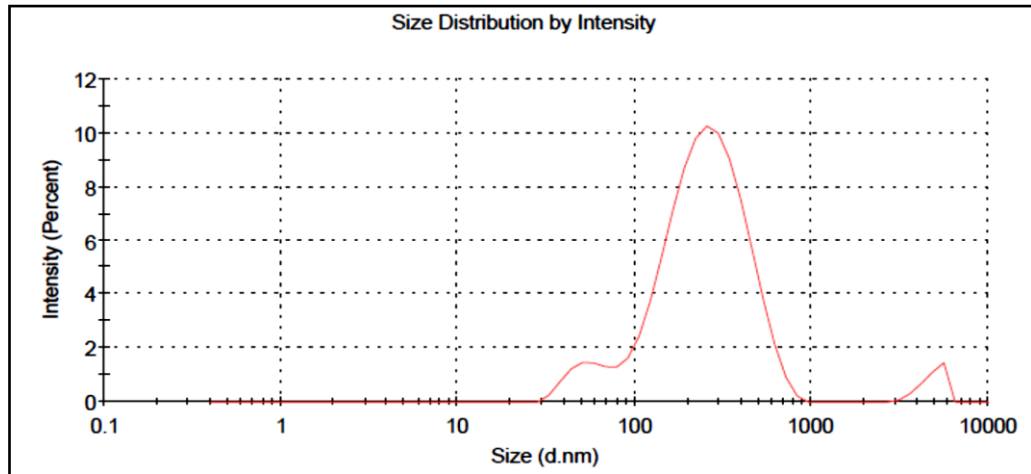


Figure 2A Intensity based Nanocarrier size distribution of batch F1 (PDI: 0.36)

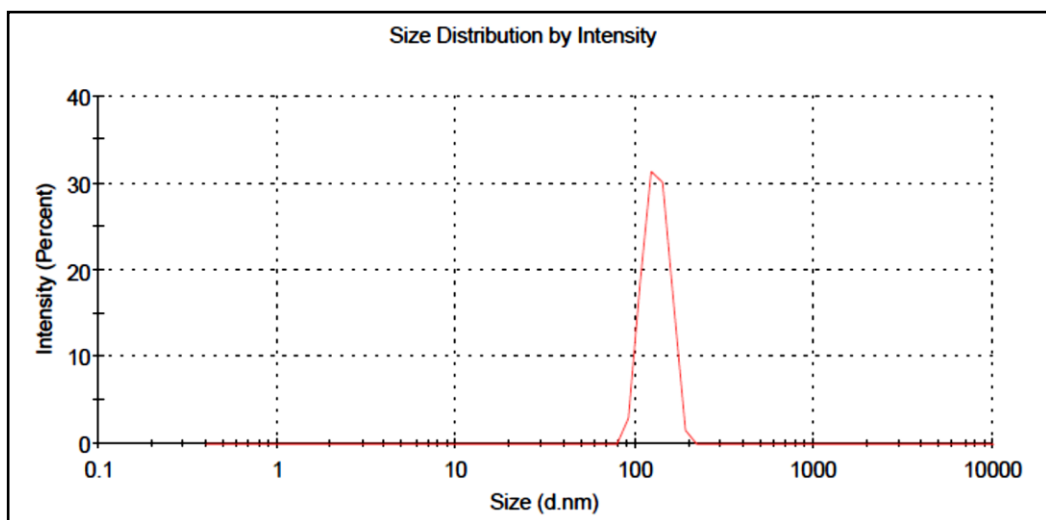


Figure 2B Intensity based Nanocarrier size distribution of batch F2 (PDI: 0.01)

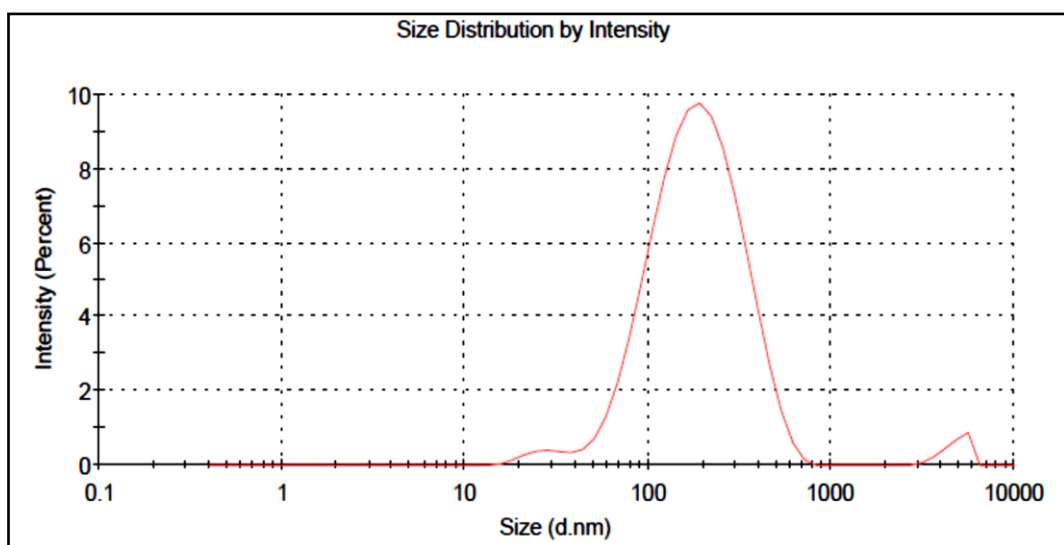


Figure 2C Intensity based Nanocarrier size distribution of batch F3 (PDI: 0.21)

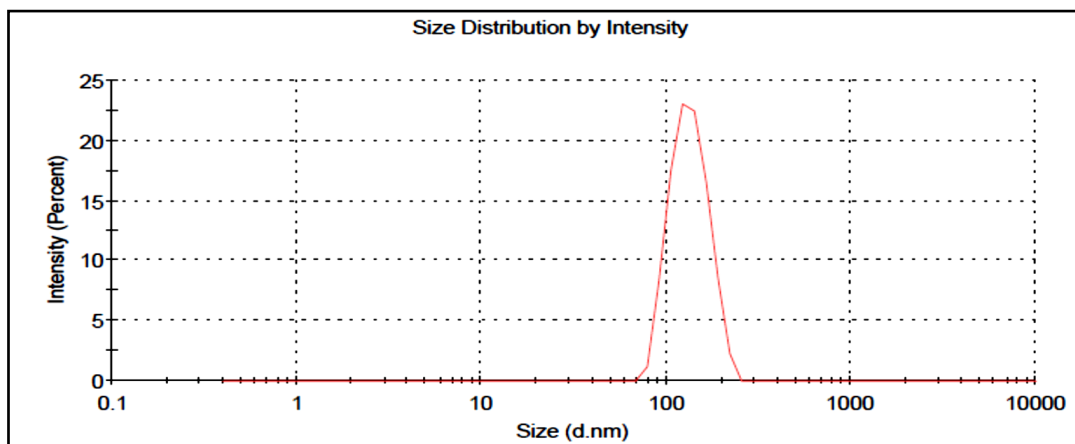


Figure 2D Intensity based Nanocarrier size distribution of batch F4 (PDI: 0.05)

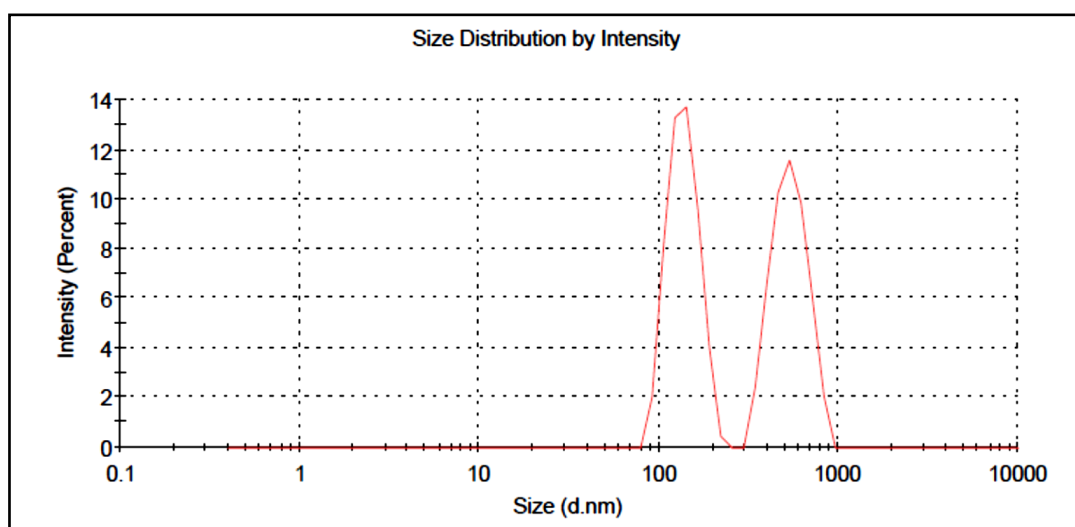


Figure 2E Intensity based Nanocarrier size distribution of batch F5 (PDI: 0.37)

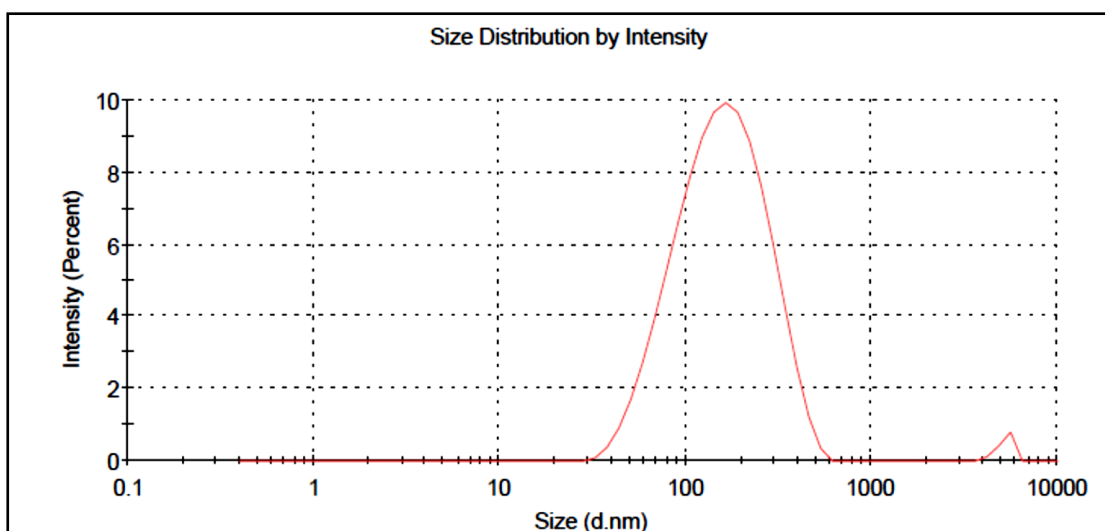


Figure 2F Intensity based Nanocarrier size distribution of batch F6 (PDI: 0.21)

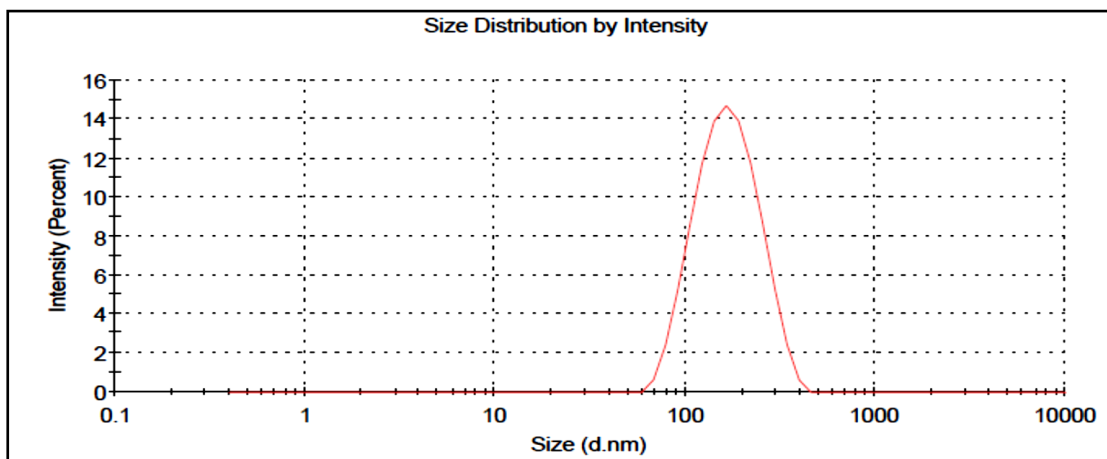


Figure 2G Intensity based Nanocarrier size distribution of batch F7 (PDI: 0.14)

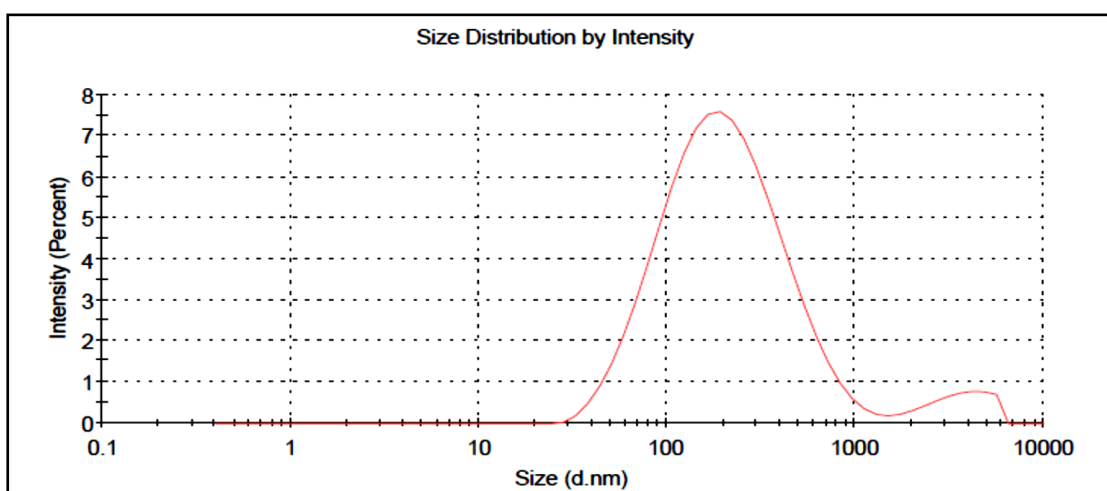


Figure 2H Intensity based Nanocarrier size distribution of batch F8 (PDI: 0.36)

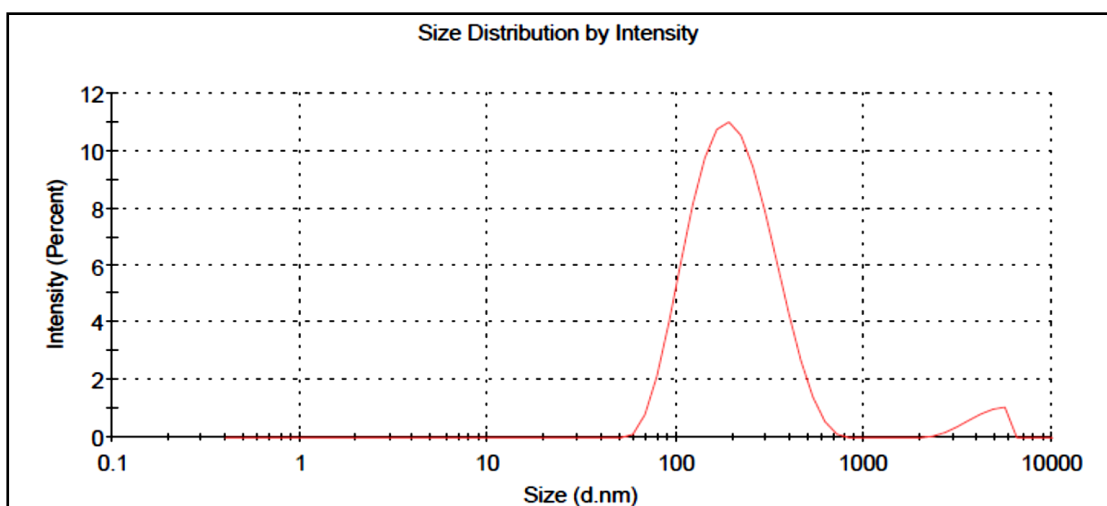


Figure 2I Intensity based Nanocarrier size distribution of batch F9 (PDI: 0.36)

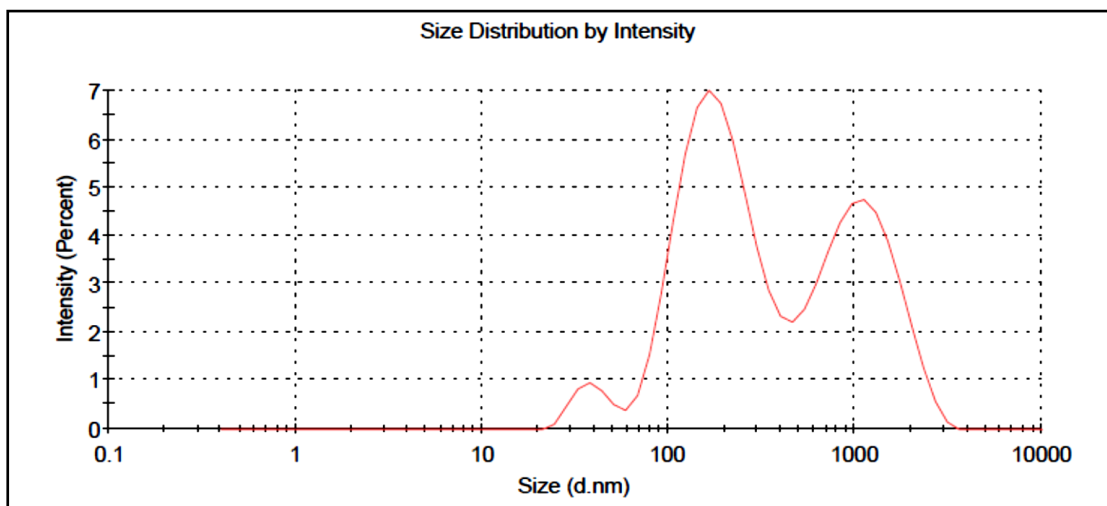


Figure 2J Intensity based Nanocarrier size distribution of batch F10 (PDI: 0.54)

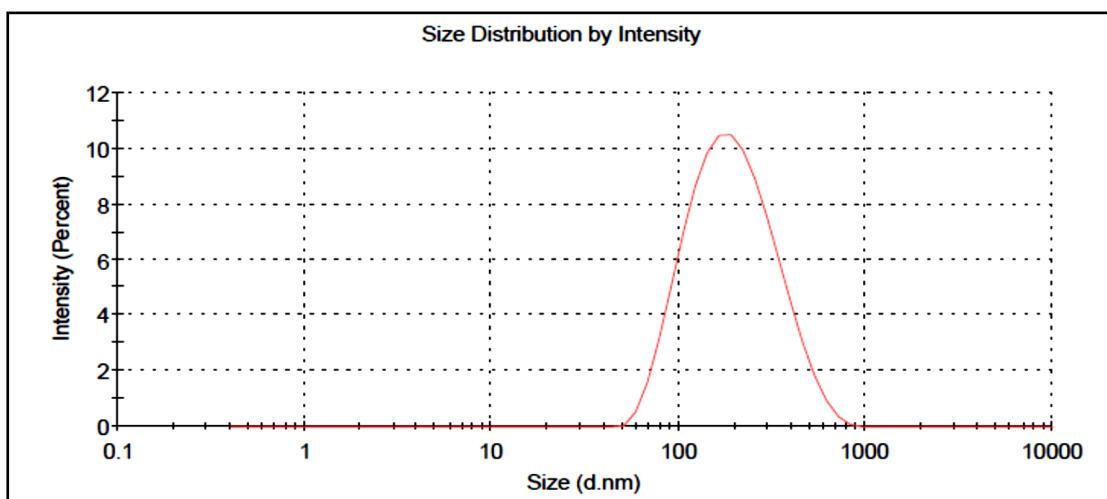


Figure 2K Intensity based Nanocarrier size distribution of batch F11 (PDI: 0.18)

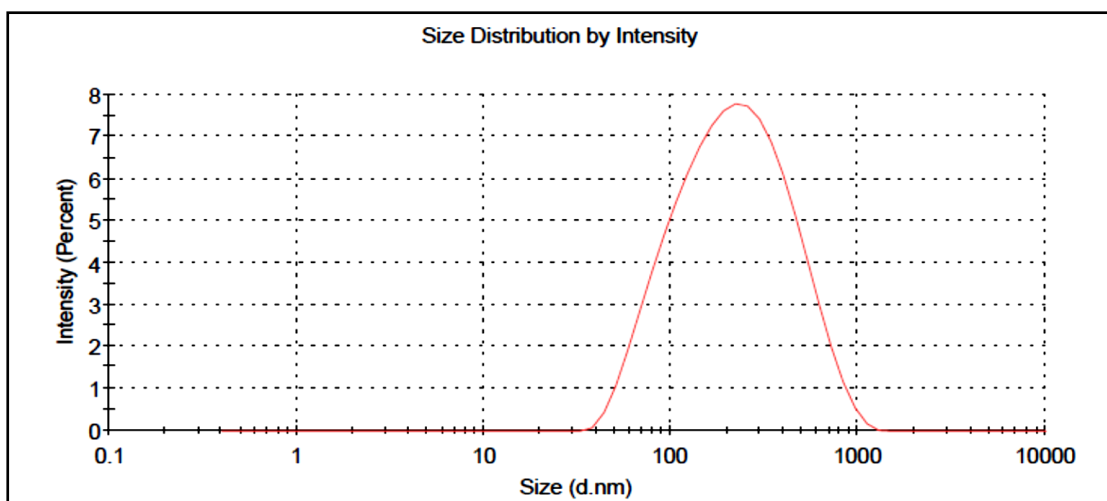


Figure 2L Intensity based Nanocarrier size distribution of batch F12 (PDI: 0.21)

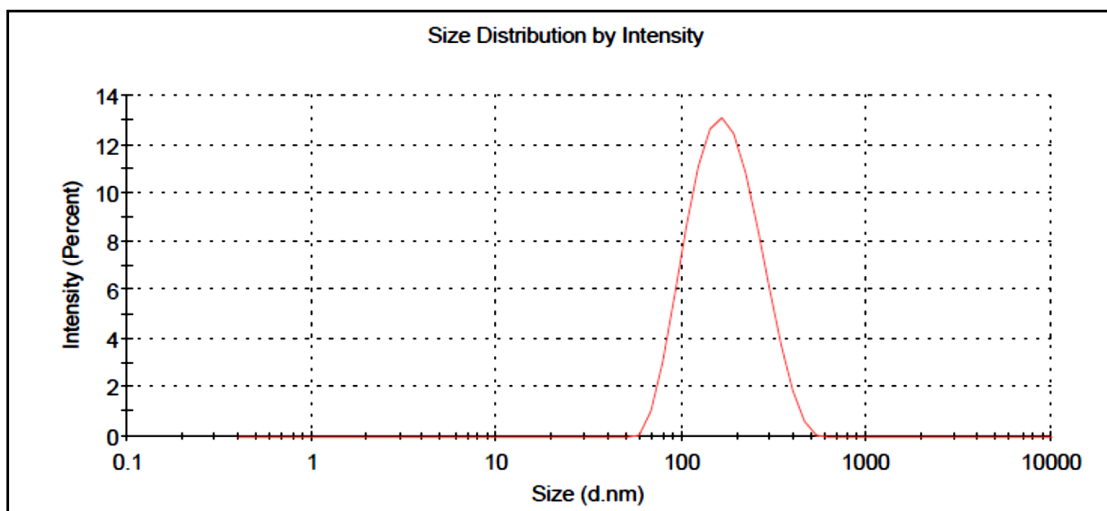


Figure 2M Intensity based Nanocarrier size distribution of batch F13 (PDI: 0.18)

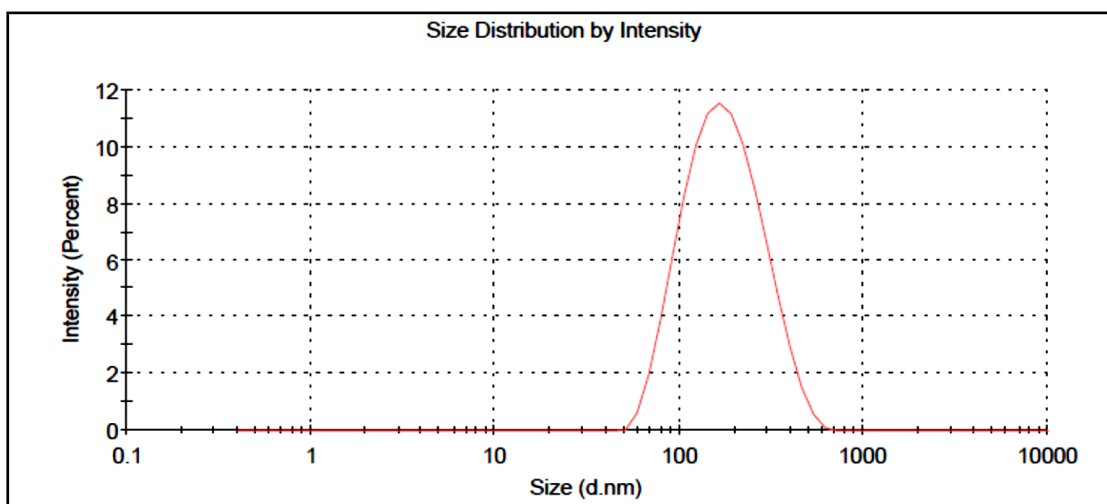


Figure 2N Intensity based Nanocarrier size distribution of batch F14 (PDI: 0.12)

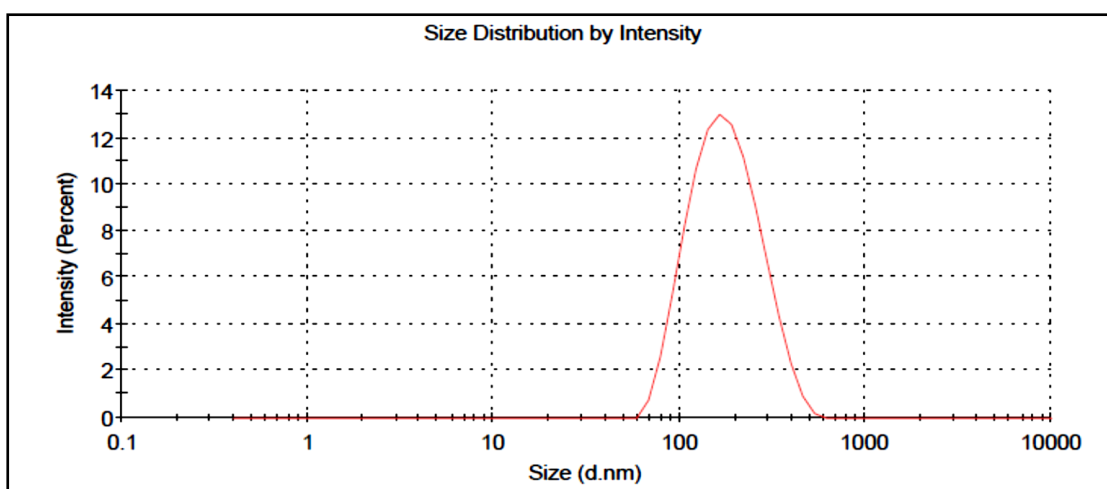


Figure 2O Intensity based Nanocarrier size distribution of batch F15 (PDI: 0.17)

5.5.3.1 Statistical analysis of response (dependent) variable 1: Nanocarrier size

(A) ANOVA results of different models

Summary of the ANOVA results for different models as shown in Table 5-8 which depicts sequential p-values and Lack of Fit p-values along with Adjusted and Predicted R-squared values for different models.

Table 5-8 Summary of ANOVA results of different models (variable 1)

Source	Sequential	Lack of Fit	Adjusted R-squared	Predicted R-squared	
	p-value	p-value			
Linear	<0.001	0.4225	0.9337	0.8989	
2FI	0.2615	0.4595	0.8711	0.8711	
Quadratic	0.0021	0.05	0.9602	0.8555	Suggested
Cubic	0.5624	-	0.9579		Aliased

Highest polynomial showing the lowest p value (<0.05) along with highest Lack of Fit p-value (>0.1) was considered for model selection. Based on the criteria quadratic model was found to be best fitted to the observed responses. Special cubic and higher models were not suitable for prediction either due to low R-squared values and/or due to higher p value as compared to quadratic model (table 5.9). Quadratic and higher models were aliased indicating the confounding of the model terms by the other implying that the predicted response would give the wrong idea of the actual response.”

Table 5-9 ANOVA results of Quadratic mixture model(variable 1)

Source	Sum of Squares	df	Mean Square	F Value	p-value	
					Prob > F	
Model	3709.58	9	412.18	38.56	0.0004	Significant
A-Lipid Concentration	2861.46	1	2861.46	267.69	< 0.0001	
B-Polymer concentration	28.50	1	28.50	2.67	0.1634	
C-lipid molar ratio	677.12	1	677.12	63.34	0.0005	
AB	5.76	1	5.76	0.54	0.4959	
AC	68.06	1	68.06	6.37	0.0500	
BC	0.023	1	0.023	0.002	0.9652	
A ²	27.42	1	27.42	2.56	0.1702	

HNCs formulation

B ²	6.48	1	6.48	0.61	0.4714	
C ²	34.35	1	34.35	3.21	0.1330	
Residual	53.45	5	10.69			
Lack of Fit	30.81	3	10.27	0.91	0.5624	Not Significant
Pure Error	22.64	2	11.32			
Cor Total	3763.03	14				

The ANOVA table revealed that the effect of factors was significant and hence the model is significant for the nanocarrier size. The F value was highest for the factor A (267.69.54), i.e. increasing lipid concentration would increase the nanocarrier size in linear manner. Other two factors such as B (Polymer concentration) and C (Lipid Molar ratio) have low effect on nanocarrier size compared to lipid concentration which can also be observed from surface plots.

The Model F-value of 38.56 implies the model is significant. There is only a 0.01% chance that a "Model F-Value" this large could occur due to noise. Values of "Prob > F" less than 0.0500 indicate model terms are significant. In this case A, C, AC are significant model terms. Values greater than 0.1000 indicate the model terms are not significant. The "Lack of Fit F-value" of 0.91 implies the Lack of Fit is not significant relative to the pure error. There is a 56.24 % chance that a "Lack of Fit F-value" this large could occur due to noise. Non-significant lack of fit is good -- we want the model to fit. Among the variables affecting nanocarrier size, Lipid concentration has maximum effect on particle size. In addition, from the actual v/s predicated plot for nanocarrier size shows a R² of which is quite good correlation.

Table 5-10 Summary of ANOVA results for nanocarrier size

Parameters	Results	Parameters	Results
Std Deviation	3.27	R-Squared	0.9858
Mean	157.67	Adjusted R-Squared	0.9602
C.V. %	2.07	Predicted R-Squared	0.8555
PRESS	543.86	Adeq. Precision	21.956

The "Pred R-Squared" of 0.8555 is in reasonable agreement with the "Adj R-Squared" of 0.9602. i.e. the difference is less than 0.1. This may indicate a

lesser block effect on model and/or data. "Adeq Precision" measures the signal to noise ratio. A ratio greater than 4 is desirable. The ratio of 21.956 indicates an adequate signal. This model can be used to navigate the design space.

(B) Model diagnostics plots

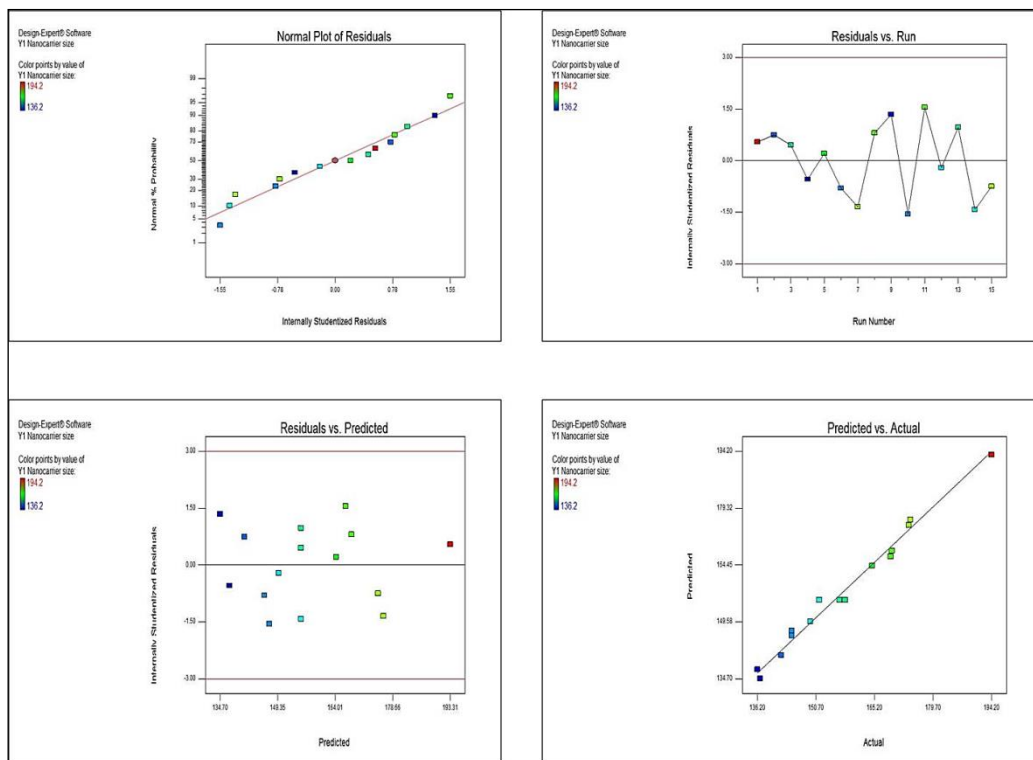


Figure 5-3 Model diagnostic plots for Nanocarrier size

Various diagnostic plots for evaluation of the model are shown in Figure 5-3. The normal probability plot (normal plot of residuals) which shows whether the residuals follows a normal distribution or not and helps identify any specific patterns in the residuals indicative of requirement of transformations i.e. “S-shaped” curve, etc. normal plot for the current data show that data follows a straight line inferring the normal distribution of the residuals.

Residuals vs. predicted response (ascending values) plot tests if variance is distributed over the design constantly i.e. variance is not associated with the factor values as megaphone patterns (pattern like sign > or <) which indicate either decreasing or increasing residuals with increasing the factor values. This is a plot of the residuals versus the ascending predicted response values.

Residual vs. run order plots the residuals against the experimental run order i.e. order in which the experiments have been carried out. The plot with a random

HNCs formulation

scatter of residuals indicate there is no time dependent changes in the residuals, i.e. there is absence of any time dependent variable among the variables selected or among the variables which has been not included in the DoE. If there is such Random scattered plot of residuals in the current analysis indicate no association of residuals with time and absence of any time dependent variable.

Predicted vs. actual plot shows correlation between the observed response values and actual response values. A good correlation between the predicted and actual values (data following a straight 45° line) shows that the model chosen for analyses of data is appropriate in predicting the responses all over the design matrix. Also, this plot helps to detect a value/ values that are not easily predicted by the model. As it can be seen from the figure, plot follows a 45° straight line indicating a close estimate of predicted values with actual values.

Box-Cox plot of $\ln(\text{residuals sum of squares})$ vs. λ for power transformation helps select any power transformation of observed response values required for fitting the model based on the best λ value and 95% confidence interval around it. Plot in Figure 5-4 shows the λ value of 1, which lies near the best λ value and within 95% confidence interval of it, indicating no requirement for any power transformation.

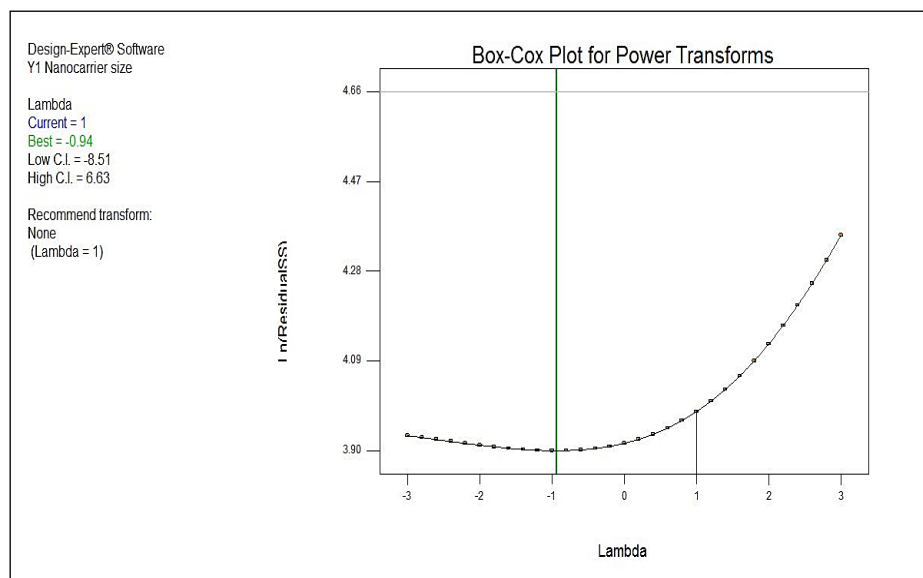


Figure 5-4 Box-cox plot for power transformation

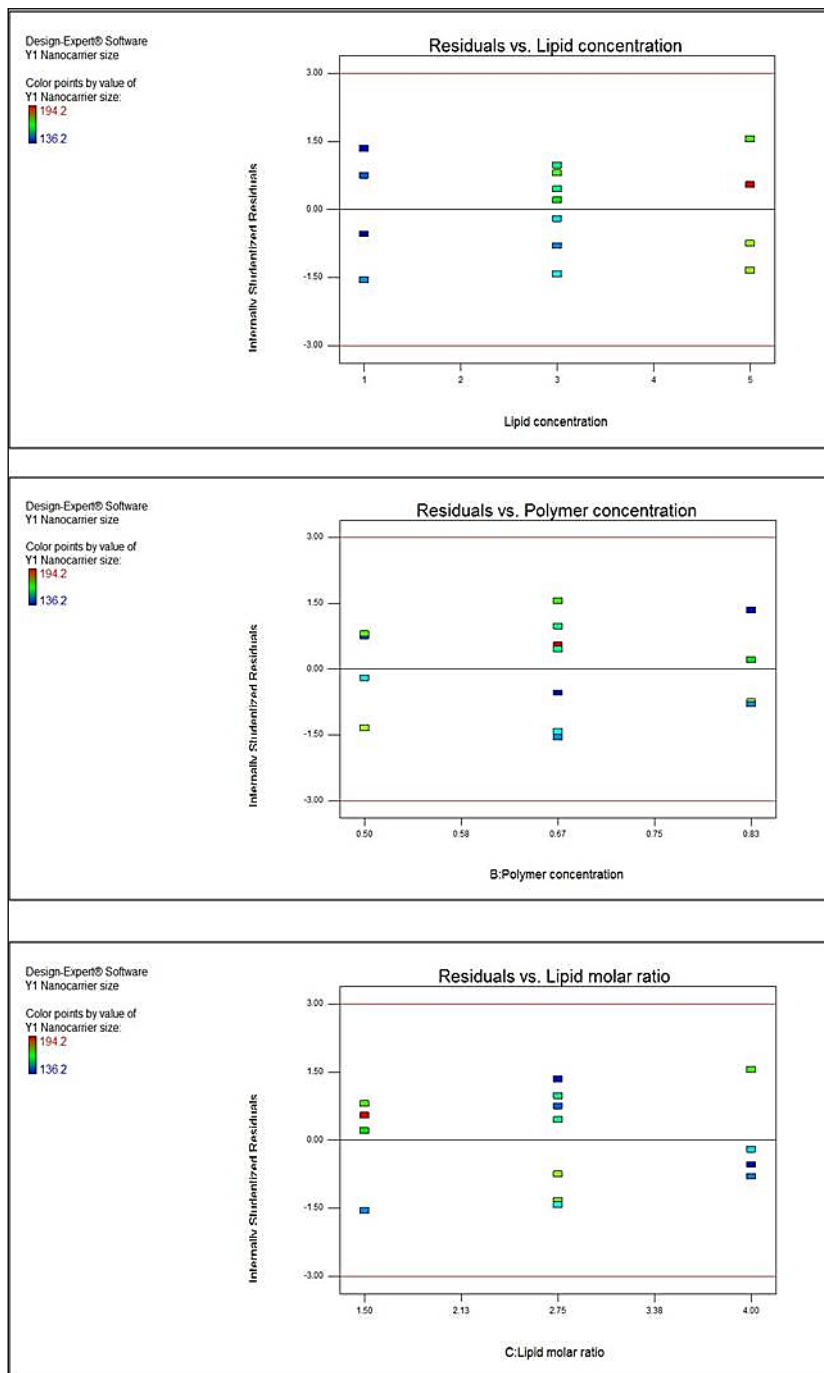


Figure 5-5 Residuals vs factor plots

Plot of residuals vs. any factor evaluated if any association is there between the variance associated with different levels of factor i.e. any specific trends (+ve or -ve curvatures) associated with increasing level of each factor. As it can be seen from the Figure 5-5 , plots for each factor shows a random scatter over the increasing levels of factors indicating that the model is effective in accounting for the variance for each factor.”

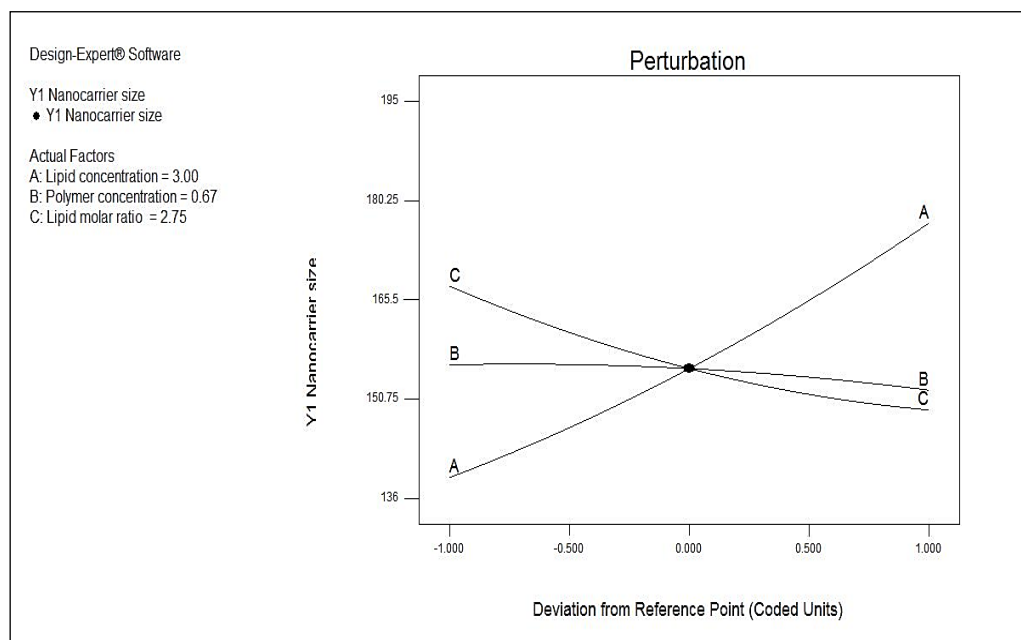


Figure 5-6 Piepel's plot on response variable 1

Piepel's plot is a trace plot showing the effect of individual factors plotting the pseudo limits of one component keeping the ratio of the changeable amounts of the each components kept constant against the response. The responses are plotted as deviations from the reference blend i.e. centroid (pseudo center point of the constrained design). As it can be seen from the plot (Figure 5-6), DPPC has positive effects on the nanocarrier size indicated by increase in the nanocarrier size along the increase in the mole% of these components.

(C) Model polts: contour (2D) plots and response surface (3D) plots

The value of ANOVA gives us idea about the factors having significant effect on nanocarrier size which is shown in contour and 3D plots. The RED area in the Figure 5-7 shows the area of maximum nanocarrier size and BLUE zone represents the area with lowest nanocarrier size.

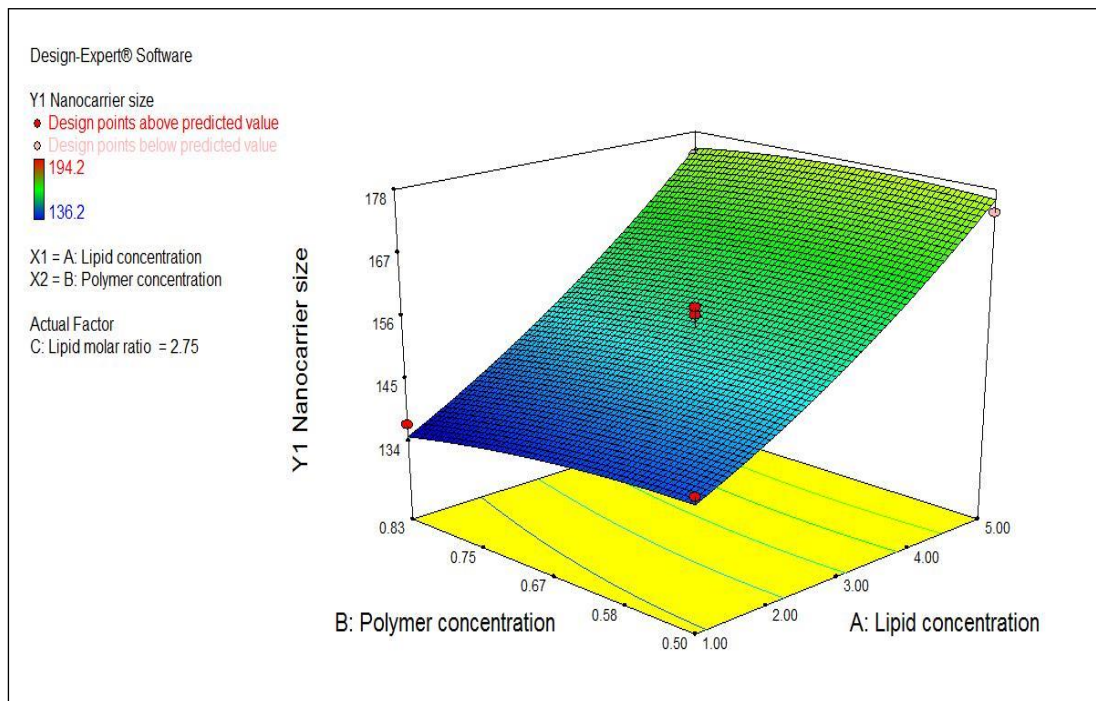


Figure 5-7 Response surface (3D) showing combined effect of Lipid concentration and polymer concentration on Nanocarrier size

From the Response surface (3D) which shows combined effect of lipid concentration and polymer concentration on nanocarrier size it was concluded that as the lipid concentration increases, there is increment in nanocarrier size and it was confirmed from the ANOVA data as the P-value for Factor –A i.e. Lipid concentration is < 0.05 which suggest this factor is significant for nanocarrier size. Also from the reduced equation it was confirmed that Lipid concentration has positive effect on Nanocarrier size. In case of Factor B i.e. Polymer concentration the P-value is > 0.05 which suggest that it is not significant to Nanocarrier size. These values are in accordance with our hypothesis of HNCs stating structural integrity and stability of formulation due to polymer.

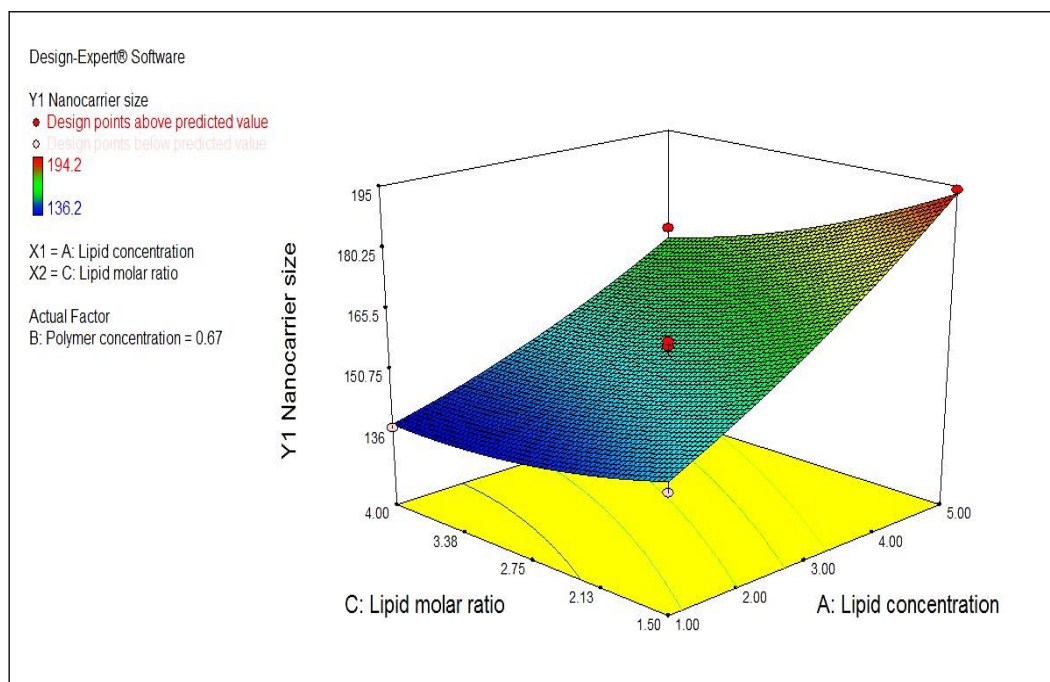


Figure 5-8 Response surface (3D) showing combined effect of Lipid concentration and Lipid molar ratio on Nanocarrier size

From the Response surface (3D) which shows combined effect of lipid concentration and Lipid molar ratio on nanocarriers size it was concluded that as there is increase in concentration, there is increase in nanocarrier size and it was confirmed from the ANOVA data as the P-value for Factor –A i.e Lipid concentration is <0.05 which suggest this factor is significant for nanocarrier size. Also from the reduced equation it was confirmed that Lipid concentration has positive effect on Nanocarrier size, so as an increase in Lipid concentration will lead to increase in nanocarrier size. In case of Factor C i.e Lipid molar ratio the P-value is <0.05 which suggest that factor C is significant to Nanocarrier size it was concluded that as the lipid molar ratio increases, nanocarrier size decreases this might be due to lesser cholesterol amount as the lipid molar ratio increases. Cholesterol is used to impart optimum fluidity to lipid bilayer. Increasing cholesterol amount leads to larger size with multi modal size distribution (wider PDI) due to excess amount in bilayer packing. It fills in empty spaces among phospholipids molecules anchoring them more strongly into the structure. The combined effect of factor A and Factor C on nanocarrier size were also confirmed from the P-Value of AC which is <0.05 which clearly described that combination of this factors have significant effect on Nanocarrier size.

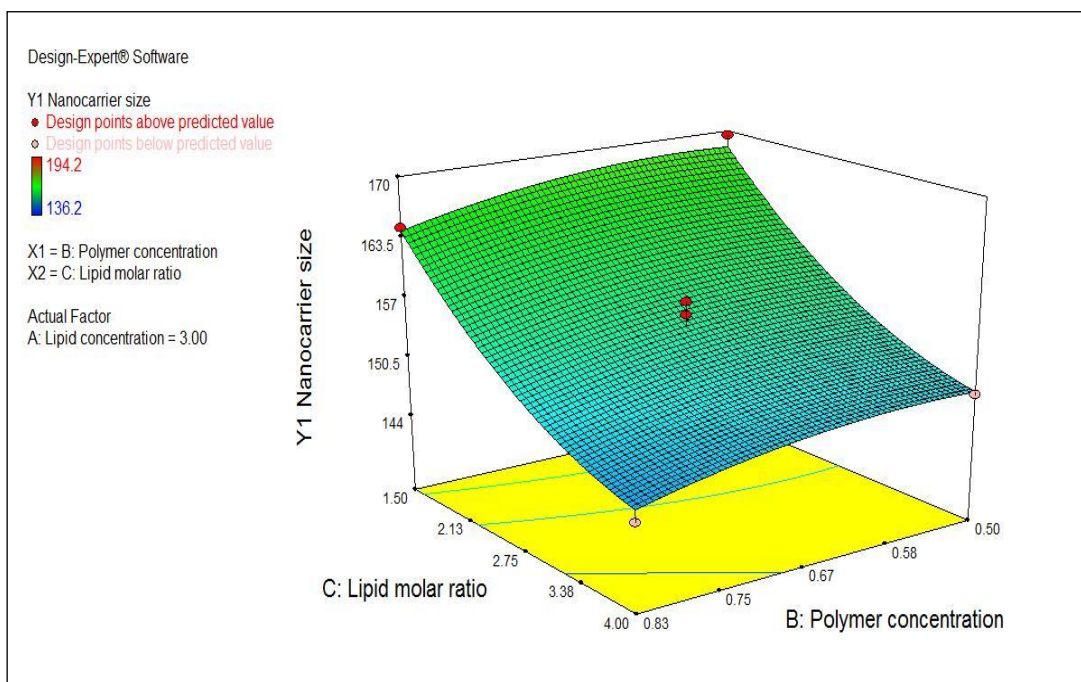


Figure 5-9 Response surface (3D) showing combined effect of Polymer concentration and Lipid molar ratio on Nanocarrier size

From the Response surface (3D) which shows combined effect of Polymer concentration and Lipid molar ratio on nanocarrier size it was concluded that as there is increase in polymer concentration there is no significant change in nanocarriers size and it was confirmed from the ANOVA data as the P-value for Factor –B i.e Polymer concentration is >0.05 which suggest this factor is not significant for nanocarrier size. In case of Factor C i.e. Lipid molar ratio the P-value is < 0.05 which suggest that factor C is significant to Nanocarrier size it was concluded that as the lipid molar ratio increases, nanocarrier size decreases this might be due to decrease in cholesterol amount as the lipid molar ratio increases.

(D) Mathematical Model for Nanocarrier Size

Final equation in terms of coded factors:

$$Y1 \text{ Nanocarrier size} = +155.30 + 18.91 * A - 1.89 * B - 9.20 * C + 1.20 * A * B - 4.13 * A * C + 0.075 * B * C + 2.73 * A^2 - 1.32 * B^2 + 3.05 * C^2$$

Reduced equation in terms of coded factors:

$$Y1 \text{ Nanocarrier size} = +155.30 + 18.91 * A - 9.20 * C - 4.13 * A * C$$

5.5.3.2 Statistical analysis of response (dependent) variable 2: Entrapment efficiency

(A) ANOVA results of different models

Summary of the ANOVA results for different models as shown in table 5.11 which depicts sequential p-values and Lack of Fit p-values along with Adjusted and Predicted R-squared values for different models.

Table 5-11 Summary of ANOVA results of different models (variable 2)

	Sequential	Lack of Fit	Adjusted	Predicted	
Source	p-value	p-value	R-squared	R-squared	
Linear	< 0.0001	0.2119	0.9373	0.9100	
2FI	0.9320	0.1542	0.9181	0.8160	
Quadratic	0.0302	0.3859	0.9744	0.8885	Suggested
Cubic	0.3859	-	0.9822		Aliased

Highest polynomial showing the lowest p value (<0.05) along with highest Lack of Fit p-value (>0.1) was considered for model selection. Based on the criteria quadratic model was found to be best fitted to the observed responses. Special cubic and higher models were not suitable for prediction either due to low R-squared values and/or due to higher p value as compared to quadratic model (table 5.11). Quadratic and higher models were aliased indicating the confounding of the model terms by the other implying that the predicted response would give the wrong idea of the actual response.” As it can be seen from table, the best model to fit the experimental results of % Entrapment efficiency is quadratic model and was chosen for further evaluation.

Table 5-12 ANOVA results of Quadratic mixture model (variable 2)

Source	Sum of Squares	df	Mean Square	F Value	p-value	
					Prob > F	
Model	1454.37	9	161.60	60.16	0.0001	Significant
A-Lipid Concentration	1241.27	1	1241.27	462.11	< 0.0001	
B-Polymer concentration	138.20	1	138.20	51.45	0.0008	
C- Lipid molar ratio	16.02	1	16.02	5.96	0.0585	
AB	0.77	1	0.77	0.29	0.6163	
AC	2.89	1	2.89	1.08	0.3471	
BC	0.00	1	0.00	0.00	1.0000	
A ²	30.95	1	30.95	11.52	0.0194	

HNCs formulation

B ²	1.78	1	1.78	0.66	0.4525	
C ²	23.78	1	23.78	8.85	0.0610	
Residual	13.43	5	2.69			
Lack of Fit	9.70	3	3.23	5.84	0.3859	Not Significant
Pure Error	3.73	2	1.86			
Cor Total	1359.53	14				

The ANOVA table revealed that the effect of factors was significant and hence the model is significant for the entrapment efficiency. The F value was highest for the factor A (462.11), i.e. increasing lipid concentration would increase the entrapment efficiency in linear manner. In this case, factor B has F value of 51.45 indicating increment in entrapment efficiency upon increasing polymer concentration. Factor C (Lipid Molar ratio) have no effect on (F value 5.96) on entrapment efficiency.

The Model F-value of 60.16 implies the model is significant. There is only a 0.01% chance that a "Model F-Value" this large could occur due to noise. Values of "Prob > F" less than 0.0500 indicate model terms are significant. In this case A, B, A² are significant model terms. Values greater than 0.1000 indicate the model terms are not significant. The "Lack of Fit F-value" of 0.38 implies the Lack of Fit is not significant relative to the pure error. There is a 38.59 % chance that a "Lack of Fit F-value" this large could occur due to noise. Non-significant lack of fit is good -- we want the model to fit. Among the variables affecting nanocarrier size, Lipid concentration has maximum effect on nanocarrier size. In addition, from the actual v/s predicated plot for nanocarrier size shows a R² of which is quite good correlation.

Table 5-13 Summary of ANOVA results for Entrapment efficiency

Parameters	Results	Parameters	Results
Std Deviation	1.64	R-Squared	0.9909
Mean	59.56	Adjusted R-Squared	0.9744
C.V. %	2.75	Predicted R-Squared	0.8885
PRESS	163.63	Adeq. Precision	25.504

The "Pred R-Squared" of 0.8885 is in reasonable agreement with the "Adj R-Squared" of 0.9744. i.e. the difference is less than 0.1. This may indicate a lesser block effect on model and/or data. "Adeq Precision" measures the signal to noise ratio. A ratio

greater than 4 is desirable. The ratio of 25.504 indicates an adequate signal. This model can be used to navigate the design space.

(B) Model diagnostics plots

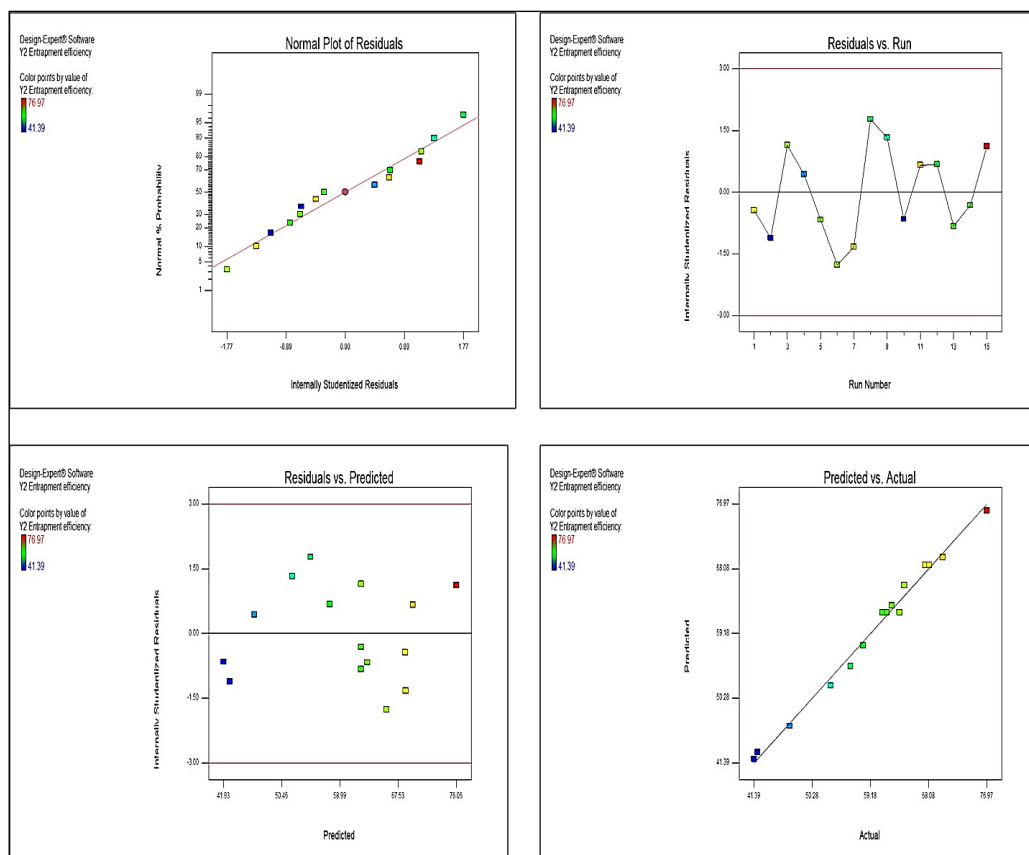


Figure 5-10 Model diagnostic plots for Entrapment efficiency

Various diagnostic plots for evaluation of the model are shown in figure 5.10. The normal probability plot (normal plot of residuals) which shows whether the residuals follows a normal distribution or not and helps identify any specific patterns in the residuals indicative of requirement of transformations i.e. “S-shaped” curve, etc. normal plot for the current data show that data follows a straight line inferring the normal distribution of the residuals.

Residuals vs. predicted response (ascending values) plot (figure 5.10) tests if variance is distributed over the design constantly i.e. variance is not associated with the factor values as megaphone patterns (pattern like sign > or <) which indicate either decreasing or increasing residuals with increasing the factor values. This is a plot of the residuals versus the ascending predicted response values.

HNCs formulation

Residual vs. run order plots the residuals against the experimental run order i.e. order in which the experiments have been carried out. The plot with a random scatter of residuals indicate there is no time dependent changes in the residuals, i.e. there is absence of any time dependent variable among the variables selected or among the variables which has been not included in the DoE. If there is such Random scattered plot of residuals in the current analysis indicate no association of residuals with time and absence of any time dependent variable.

Predicted vs. actual plot shows correlation between the observed response values and actual response values. A good correlation between the predicted and actual values (data following a straight 45° line) shows that the model chosen for analyses of data is appropriate in predicting the responses all over the design matrix. Also, this plot helps to detect a value/ values that are not easily predicted by the model. As it can be seen from the figure, plot follows a 45° straight line indicating a close estimate of predicted values with actual values.

Box-Cox plot of $\ln(\text{residuals sum of squares})$ vs. λ for power transformation helps select any power transformation of observed response values required for fitting the model based on the best λ value and 95% confidence interval around it. Plot in Figure 5.11 shows the λ value of 1, which lies near the best λ value and within 95% confidence interval of it, indicating no requirement for any power transformation.

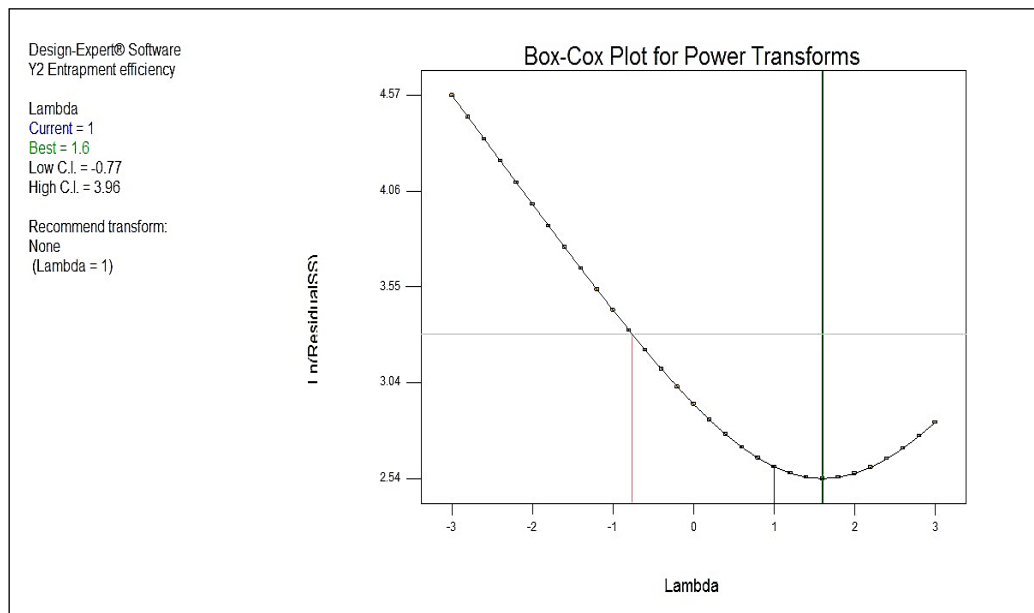


Figure 5-11 Box-cox plot for power transformation of variable 2

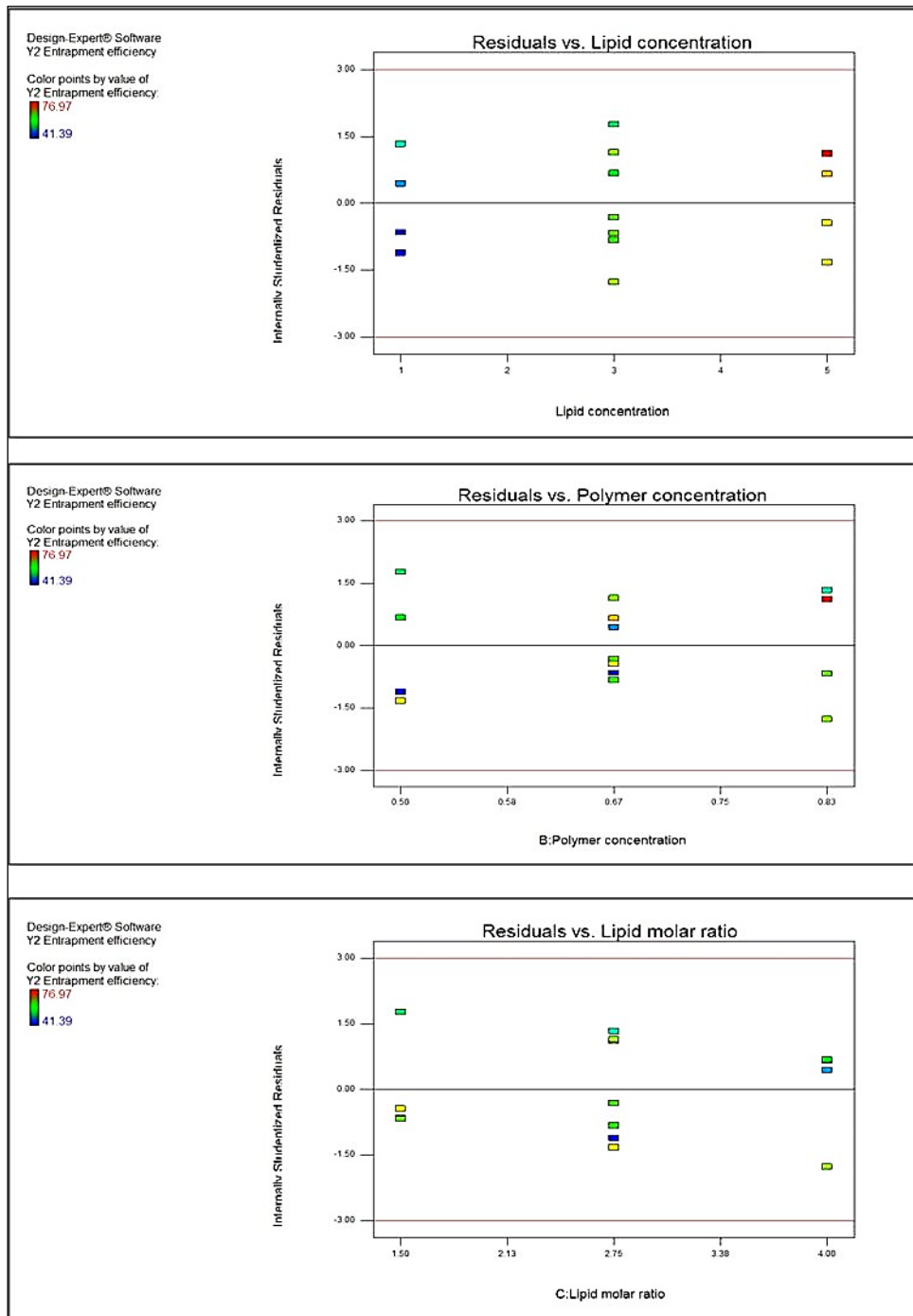


Figure 5-12 Residuals vs factor plots of variable 2

Plot of residuals vs. any factor evaluated if any association is there between the variance associated with different levels of factor i.e. any specific trends (+ve or -ve curvatures) associated with increasing level of each factor. As it can be seen from the Figure 5.12 , plots for each factor shows a random scatter over the increasing levels of factors indicating that the model is effective in accounting for the variance for each factor.”

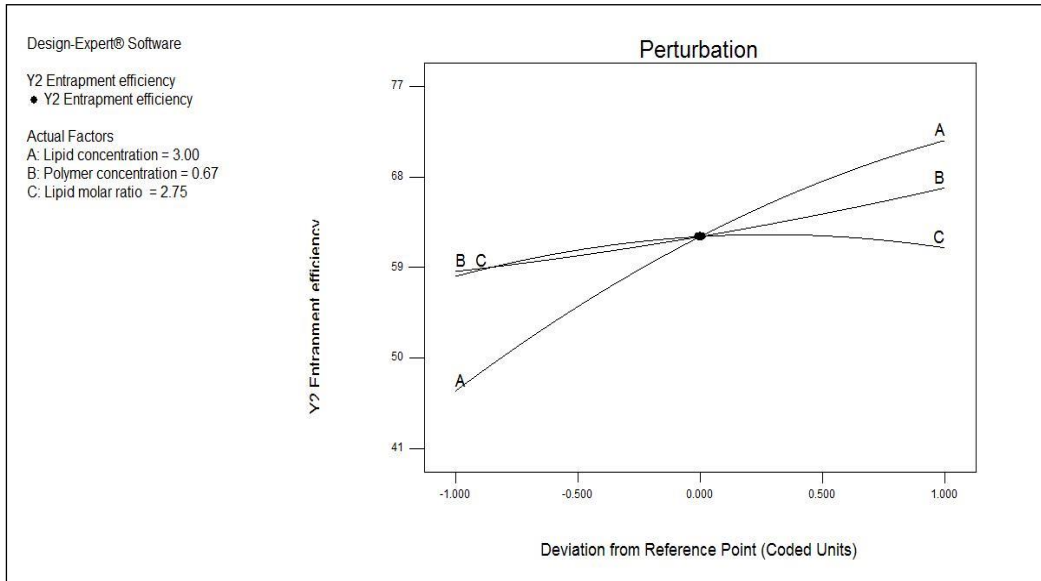


Figure 5-13 Piepel's plot on response of variable 2

Piepel's plot is a trace plot showing the effect of individual factors plotting the pseudo limits of one component keeping the ratio of the changeable amounts of the each components kept constant against the response. The responses are plotted as deviations from the reference blend i.e. centroid (pseudo center point of the constrained design). As it can be seen from the plot (Figure 5.13), increment in lipid concentration and polymer concentration has positive effects on the entrapment efficiency indicated by increase in entrapment efficiency.

(C) Model plots: Response surface (3D) plots

The value of ANOVA gives us idea about the factors having significant effect on entrapment efficiency which is shown in contour and 3D plots. The RED area in the fig 5.13 shows the area of maximum entrapment efficiency and BLUE zone represents the area with lowest entrapment efficiency.

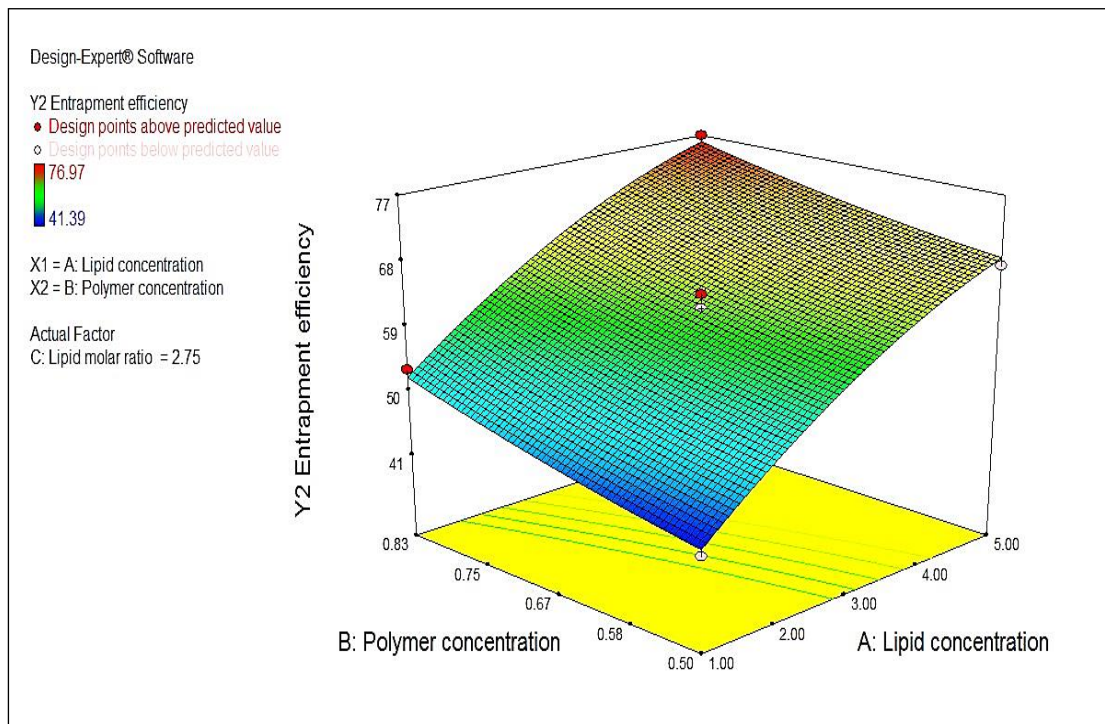


Figure 5-14 Response surface (3D) showing combined effect of Lipid concentration and polymer concentration on %Entrapment efficiency

From the Response surface (3D) which shows combined effect of lipid concentration and polymer concentration on % Entrapment efficiency it was concluded that as there is increase in Lipid concentration & Polymer concentration there is increase in % Entrapment efficiency and it was confirmed from the ANOVA data as the P-value for Factor-A i.e Lipid concentration and Factor -B i.e Polymer concentration is <0.05 which suggest this both factors are significant for % Entrapment efficiency. Also, from the reduced equation it was confirmed that Lipid concentration & Polymer concentration has positive effect on % Entrapment efficiency, so as an increase in Lipid concentration & Polymer concentration will lead to increase in % Entrapment efficiency. The increment in cisplatin caprylate entrapment efficiency is due to amphiphilic nature of block co-polymer PEG-PLA in which PLA chains confer hydrophobicity to HNCs and block co-polymer can accommodate cisplatin caprylate within its matrix inside HNCs. This results is in agreement with Cryo-TEM results which revealed formation of polymeric amorphous region of solid matrix core

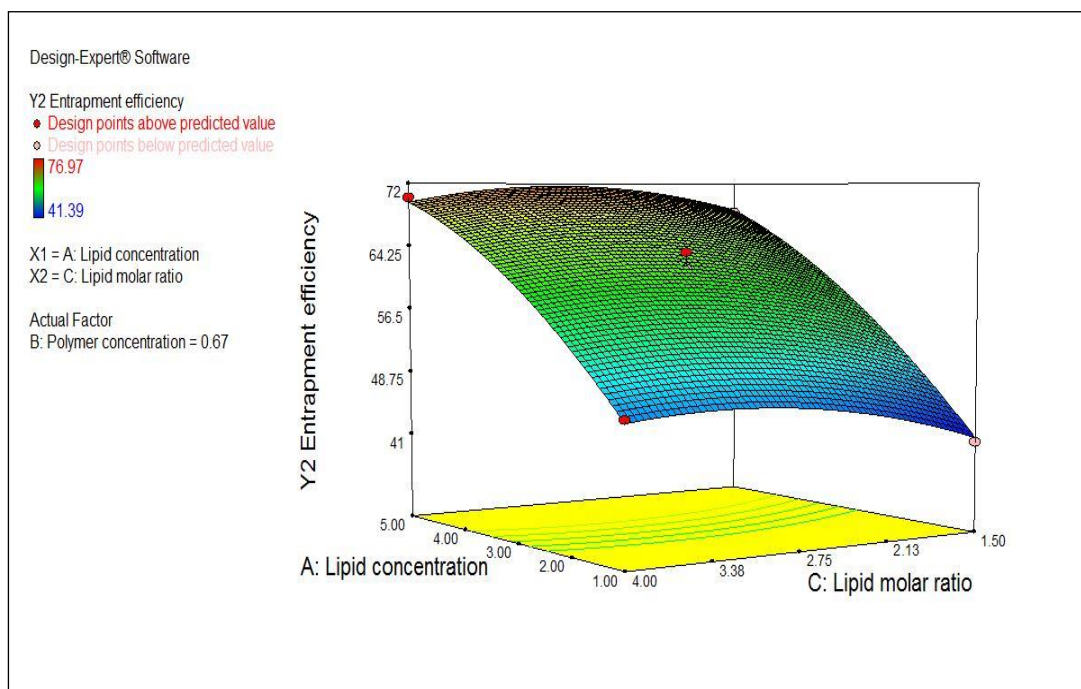


Figure 5-15 Response surface (3D) showing combined effect of Lipid concentration and Lipid molar ratio on %Entrapment efficiency

From the Response surface (3D) which shows combined effect of lipid concentration and Lipid molar ratio on % Entrapment efficiency it was concluded that as there is increase in Lipid concentration there is increase in % Entrapment efficiency and it was confirmed from the ANOVA data as the P-value for Factor-A i.e Lipid concentration is <0.05 which suggest this factor is significant for % Entrapment efficiency. Also, from the reduced equation it was confirmed that Lipid concentration has positive effect on % Entrapment efficiency so increasing lipid concentration will lead to increment in %Entrapment efficiency. In case of Factor-C i.e Lipid molar ratio the P-value is > 0.05 which suggested that it is not significant to % Entrapment efficiency.

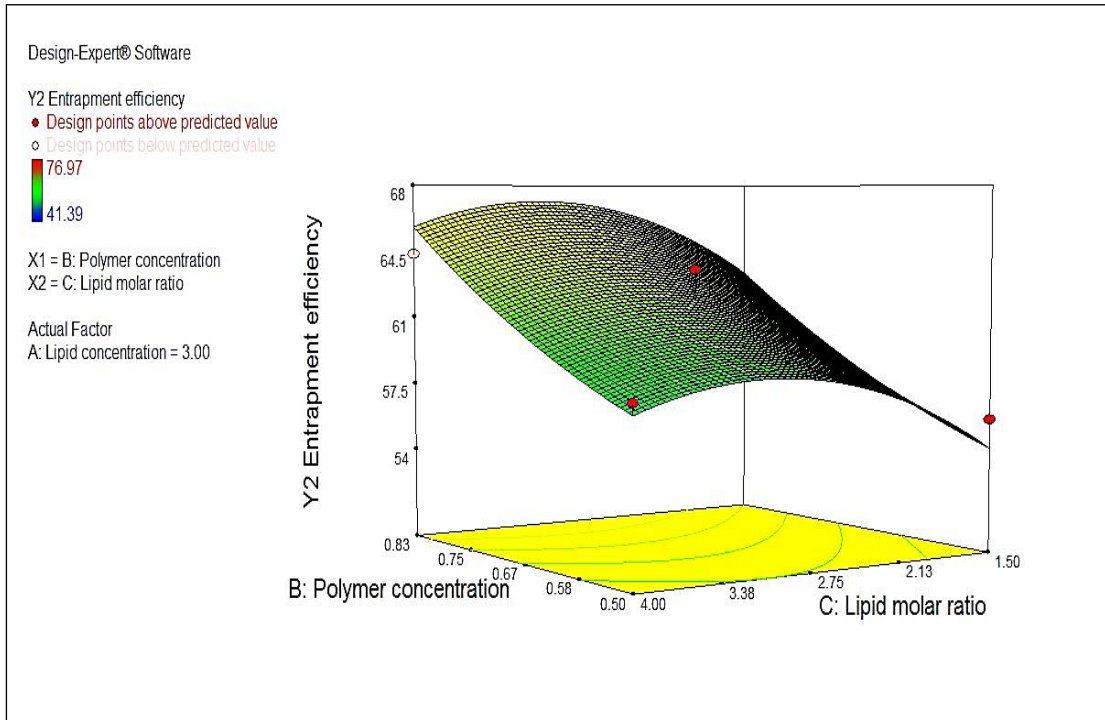


Figure 5-16 Response surface (3D) showing combined effect of Polymer concentration and Lipid molar ratio on %Entrapment efficiency

From the Response surface (3D) which shows combined effect of Polymer concentration and Lipid molar ratio on % Entrapment efficiency it was concluded that as there is increase in Polymer concentration there is increase in %Entrapment efficiency and it was confirmed from the ANOVA data as the P-value for Factor-B i.e Polymer concentration is <0.05 which suggest this factor is significant for %Entrapment efficiency. Also from the reduced equation it was confirmed that Polymer concentration has positive effect on % Entrapment efficiency so increasing Polymer concentration will lead to increment in %Entrapment efficiency. In case of Factor-C i.e Lipid molar ratio the P-value is >0.05 which suggested that it is not significant to %Entrapment efficiency.

(D) Mathematical Model for Entrapment efficiency

Final equation in terms of coded factors:

$$\% \text{Entrapment efficiency} = +62.08 + 12.46 * A + 4.16 * B + 1.41 * C - 0.44 * A * B - 0.85 * A * C - 0.00 * B * C - 2.90 * A^2 + 0.69 * B^2 - 2.54 * C^2$$

Reduced equation in term of coded factors:

$$\% \text{Entrapment efficiency} = +62.08 + 12.46 * A + 4.16 * B - 2.90 * A^2$$

5.5.4 Desirability plot and overall plot for optimization

A desirability plot gives optimum value of variables so as to be obtained desired responses. Desirability plot was generated using Design Expert 7.0.0. Parameters for the desirability batch were shown in table.5.11.

Table 5-14 Variables for desirability plot and goals for response

Name	Goal	Limit	Limit
A Lipid Concentration(mM)	In range	1.0	5.0
B Polymer Concentration (mg/ml)	In range	0.50	0.83
C Lipid molar ratio	In range	1.50	4.0
Nanocarrier size (nm)	Target-160	136.2	194.2
Entrapment Efficiency	Maximize	41.39	76.97

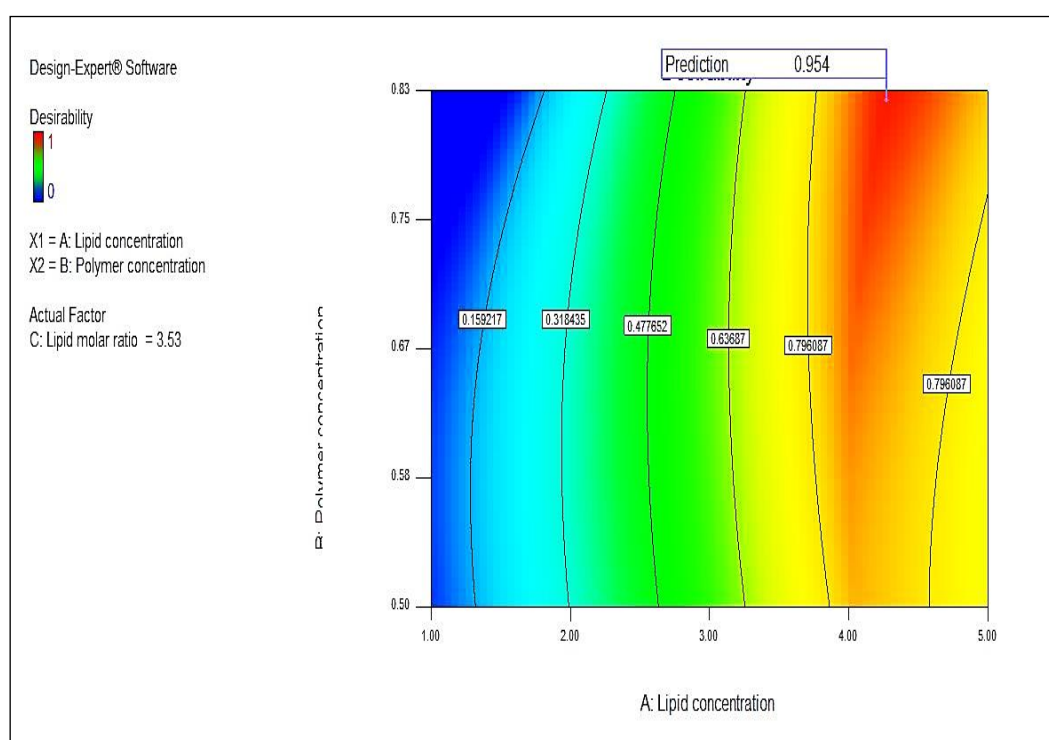


Figure 5-17 Desirability Plot

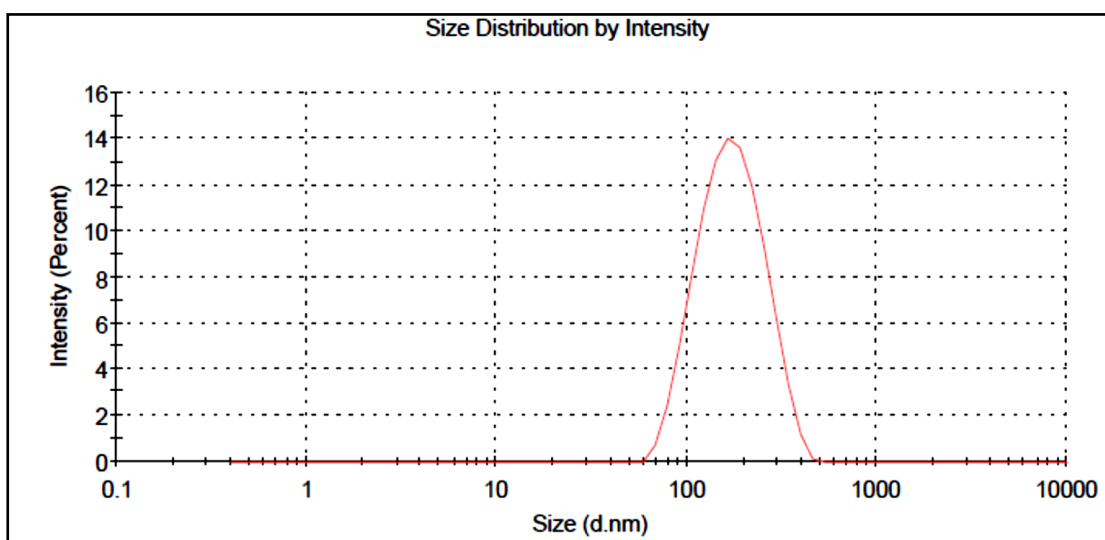
Table 5-15 Optimized batch (R1) of the HNCs

Exp. Run	Lipid Concentration (mM)	Polymer Concentration (mg/ml)	Lipid molar ratio	Size (nm)	Entrapment Efficiency (%)	Desirability
1	4.28	0.82	3.53	162.2±3.45	71.53±2.12	0.95

Table 5-16 Evaluation of desirability batch

Response	Experimental Value	Predicted Value
Nanocarrier size (nm)	162.2±3.45	159.99
% Entrapment efficiency (%)	71.53±2.12	72.77

The obtained results demonstrate the suitability of predicted desirability plot of optimized formulation (R1). The obtained value of response was very close to predicted value of responses. This shows that the optimized formulation predicted by software holds true for practical purpose. Size analysis report by Malvern zetasizerNano ZS is given in figure 5.18.

**Figure 5-18 Intensity based Nanocarrier size distribution of optimized batch Batch R1**

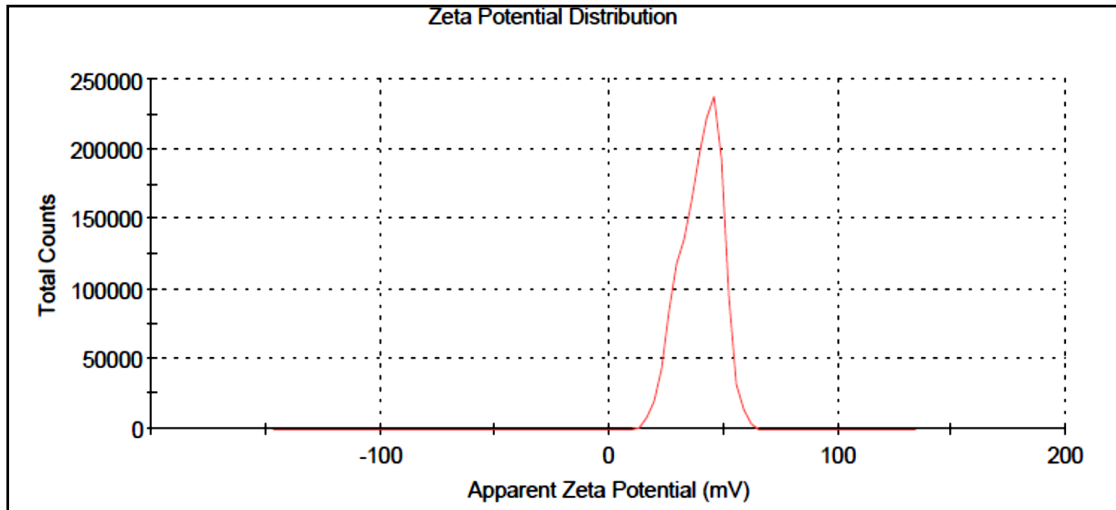


Figure 5-19 Zeta potential distribution of Batch optimized batch R1

Overlay Plot for predicted design space

Design expert was used for two responses: Nanocarrier size and % EE, it is necessary to obtain a region that provides optimum value of factors. Overlay plot can be obtained by superimposing contour plot of both responses which displaces area of feasible response values in the factor space. The region highlighted in yellow color is the area in which a slight variation in the critical variables won't affect the final response and the response will be in desired range. Region that do not fit the optimization criteria are shaded gray while design space which is accepted colored yellow.

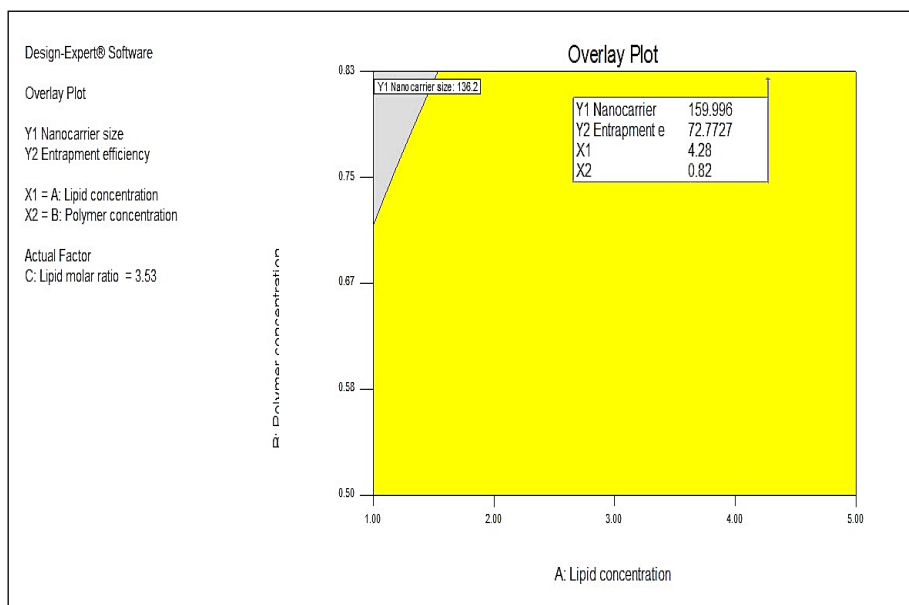


Figure 5-20 Overlay Plot for Design space

Analysis of Design Space

It is very important to analyze the design space for robustness. This gives idea about reproducibility of results when formulation development is done in that particular design space. For analyzing the design space robustness, three formulations were flagged randomly in the plotted design space. The formulation was developed according to the provided values of factors and the observed responses were compared with predicted value of responses.

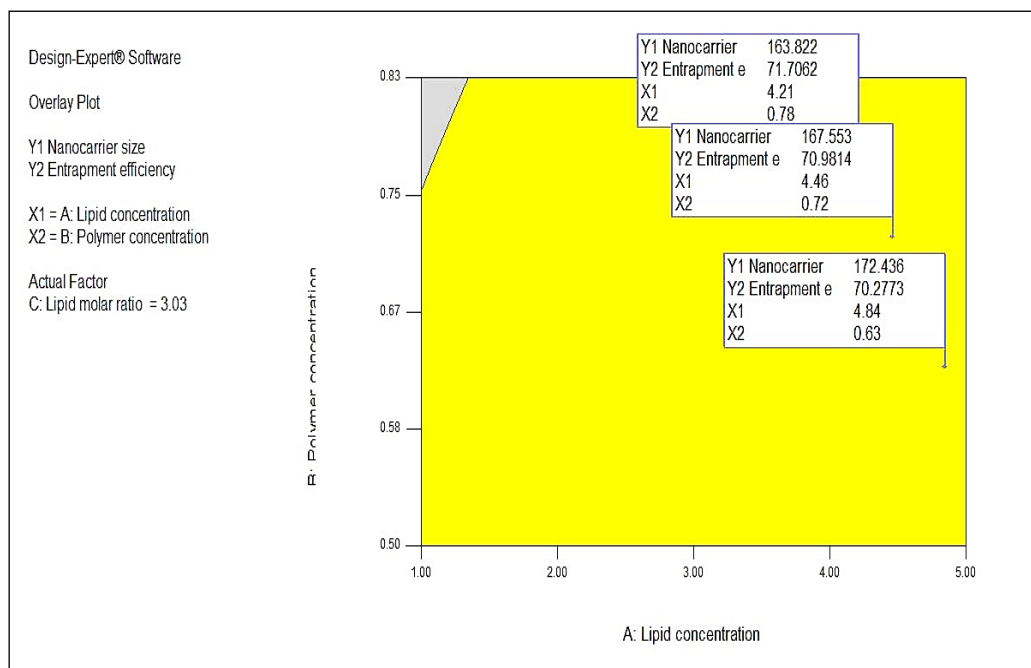


Figure 5-21 Analysis of Design Space

Table 5-17 Check point batch analysis

Formulation	Parameter	Predicted	Observed	Error
1.	Nanocarrier Size	163.82	165.1	+1.28
	% EE	71.70	68.12	-3.58
2.	Nanocarrier Size	167.55	165.8	-1.75
	% EE	70.98	67.60	-3.38
3.	Nanocarrier Size	172.43	169.4	-3.03
	% EE	70.27	68.50	-1.77

From the robustness analysis, we observed that the observed responses were inside the boundary and the difference between predicted value and observed value was not significant.

Point Prediction & Confirmation

Table 5-18 shows predicted responses for the solution selected above along with the Standard deviation and 95 % confidence interval of the responses. Confirmation of the responses was done by carrying out the experiment using the selected factor values in triplicate. Table 5-16 shows and confirms that experimental and predicted values are in good agreement concluding the suitability of the selected model for optimization.

Table 5-18 Predicted responses for selected solution along with standard deviation

Response	Predicted Mean	Observed mean	Std Dev	SE mean	95% CI low	95% CI high
Nanocarrier Size	159.99	162.2	2.21	2.25	152.04	168.04
% EE	72.77	71.53	1.24	1.29	69.37	76.67

Optimized batch (R1) of Cisplatin caprylate loaded HNCs from Design Expert

Table 5-19 Composition and Parameters for optimized batch (R1) Cisplatin caprylate loaded HNCs

Sr. No.	Components	Optimized Parameter
1	Lipid Concentration (mM)	4.28
2	Polymer Concentration (mg/ml)	0.82
3	Lipid molar ratio	3.53
4	Solvent evaporation temperature(°C)	45
5	Solvent evaporation time (mins)	30
6	Vacuum condition (mm-Hg)	400
7	Rotation speed (rpm)	100
8	Extrusion cycles	3

Characterization of optimized batch (R1): Cisplatin caprylate loaded HNCs formulation

Following evaluation tests (5.5.5 to 5.5.14) were carried out to assess optimized batch (R1) i.e. Cisplatin caprylate loaded HNCs formulation.

5.5.5 Nanocarrier size analysis by Dynamic light scattering (DLS)

To have therapeutic potential as a drug delivery system, drug-loaded HNCs must possess a narrow size distribution of Sub-micrometer mean, together with a biocompatible zeta potential and an efficient drug loading. In the present study the

Nanocarrier size obtained was in the range of 155 to 165 nm ($162.2 \text{ nm} \pm 3.45 \text{ nm}$) with very good polydispersity index of 0.098 (Figure 5-18).

The Nanocarrier Size is an important particle property, as it can influence the biopharmaceutical properties of the particle preparations. The biodistribution of the particles may also depend on the Particle Size. Endocytosis of the particles, is size dependent. The particle uptake is reported to be the size dependent phenomena, where the small sized particles could be efficiently taken up as compared to the bigger sized particles. For Cancer cells, particle size is important to target EPR (Enhanced Permeability and Retention) effect which plays very crucial role in targeting.

5.5.6 Zeta potential analysis

The zeta potential of HNCs was found to be $+43.18 \text{ mV} \pm 1.83 \text{ mV}$ (Figure 5-19) which is due to presence of cationic lipid i.e DOTAP. Positively charged Particles will repel one other and provide stability by preventing aggregation. Cationic charge is necessary for siRNA complexation and cellular uptake.

5.5.7 Entrapment efficiency and drug loading

Assay of LPHNs:

The % assay was found to be in the range of 95-105 %.

%Entrapment efficiency:

The % entrapment efficiency was found to be 71.53 ± 2.12 (n=3) in the optimized formulation R1.

Drug loading

The drug loading was found to be 7.2 % w/w. (n=3)

5.5.8 Transmission Electron Microscopy (TEM)

For structural characterization of HNCs, negative staining with uranyl acetate in TEM was performed which stains lipid layer which was observed as a dim ring (Fig. 22a) surrounding the polymeric core. The thickness of ring is less than 20 nm. It confirms the morphology and architecture of HNCs i.e.formation of polymeric amorphous region of solid matrix core inside lipid bilayer. Polymeric core showed distinct PEG-PLA particles inside cavity of HNCs (figure 22d) with embedded matrix formation as well which strengthen the architecture of HNCs in comparison to liposomes (Fig. 22c) alone.

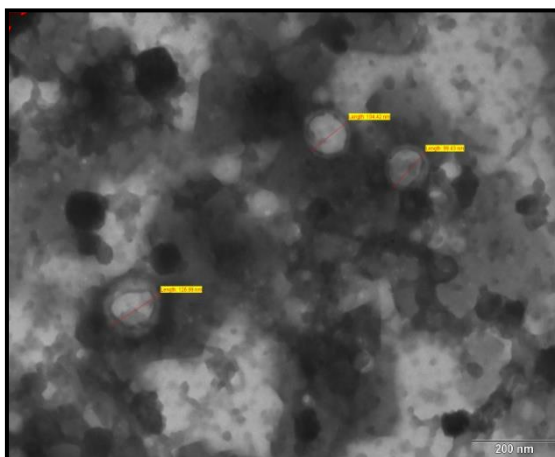


Figure 5-22 HNCs SEM negative staining

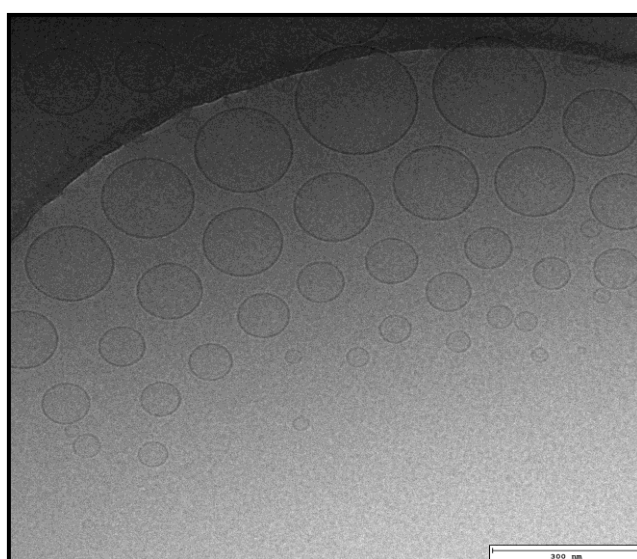


Figure 5-23 Cryo-TEM of liposomes (Batch V3)

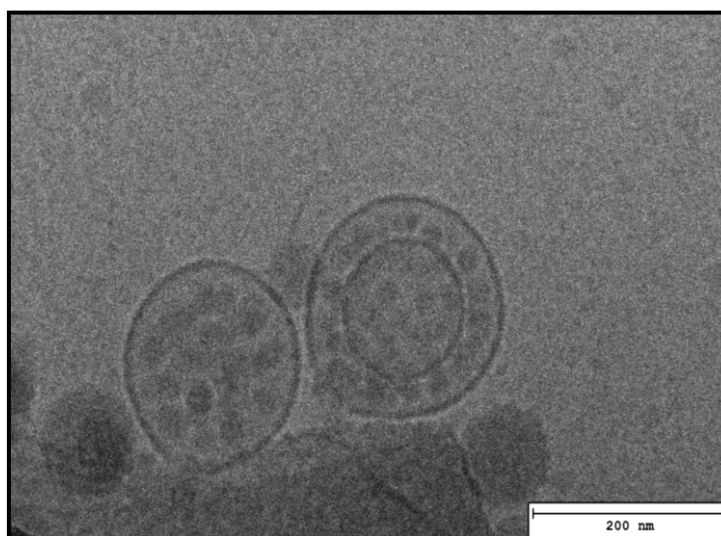


Figure 5-24 Cryo-TEM of HNCs R1

5.5.9 Scanning Electron Microscopy (SEM) Analysis

Surface visualization and shape of nanocarriers were conformed and HNCs vesicles were found to be spherical in shape with size of 170 nm approximately.

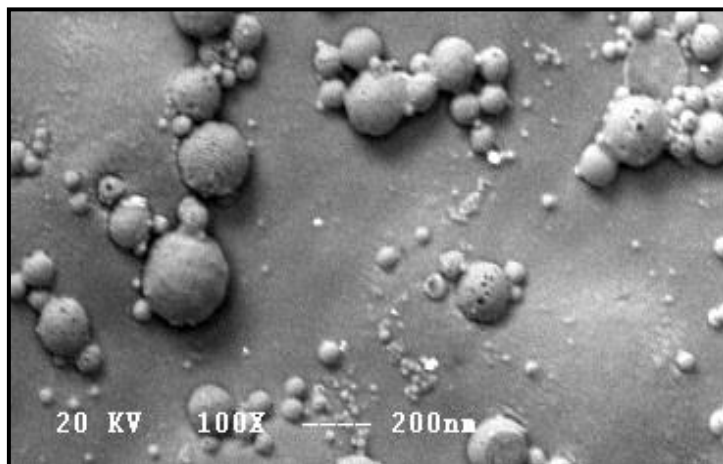


Figure 5-25 SEM image of HNCs R1

5.5.10 *In-vitro* drug release study and drug release kinetic

The drug release at pH 7.4 will give idea about Cisplatin caprylate release from HNCs in blood and inside the normal tissue. The drug release at pH 6.6 will give an idea about the Cisplatin caprylate release in cancer tissue interstitials. And drug release at pH 5.5 will give an idea about the Cisplatin caprylate release inside the cancer cells once HNCs get internalized by cancer cells. Here, Lipid coating around HNCs and polymeric core matrix of PEG-PLA retard the drug release kinetics by keeping the external dissolution fluid medium away from the polymeric matrix core thereby drug release kinetic is governed by both lipid as well as polymer's characteristics. At pH 7.4, its release was very slow showing only 15 % release within initial 10 hr time period and reached to a maximum of 27 % in the span of 3 days (Figure 5-26). This again infers that Cisplatin caprylate release in the blood as well as in normal tissues will be very low thereby a low toxicity might be conferred by the HNCs. At pH 6.6, release was found to be somewhat faster, showing 25 % release within 10 hr but then after it was slowed down. Cisplatin caprylate release from HNCs at pH 5.5 showed a drastic release pattern with 38 % release within first 10 hr and it went on increasing to around 48 % in 24 hr which indicated that 48 % Cisplatin caprylate could be released inside the cells within one day once HNCs gets

HNCs formulation

internalized by cancer cells. Endosomes and lysosomes of cancer cells (pH 5-6) would be playing important role in inducing release of cisplatin caprylate from HNCs.

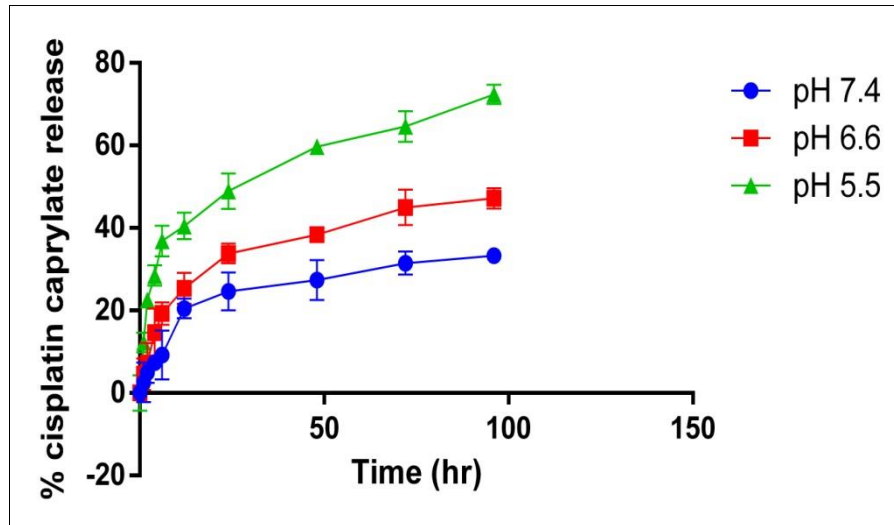


Figure 5-26 cisplatin release from HNCs

From the Kinetic model fitting analysis, it was concluded that for Cisplatin caprylate loaded HNCs the best fit was Higuchi model (Figure 5-27) with R^2 value of 0.927. This shows that the drug release is matrix diffusion controlled release process HNCs.

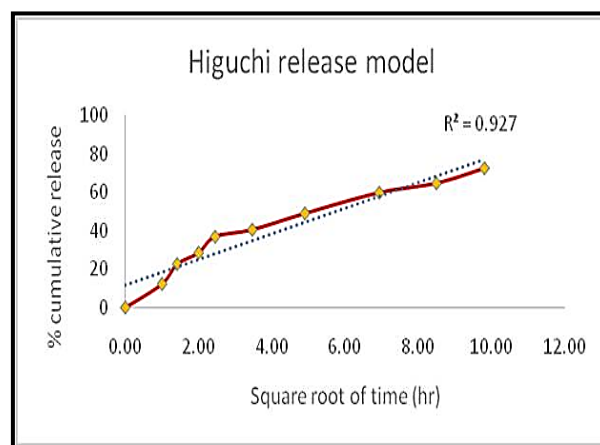


Figure 5-27 Drug release kinetic: Higuchi model

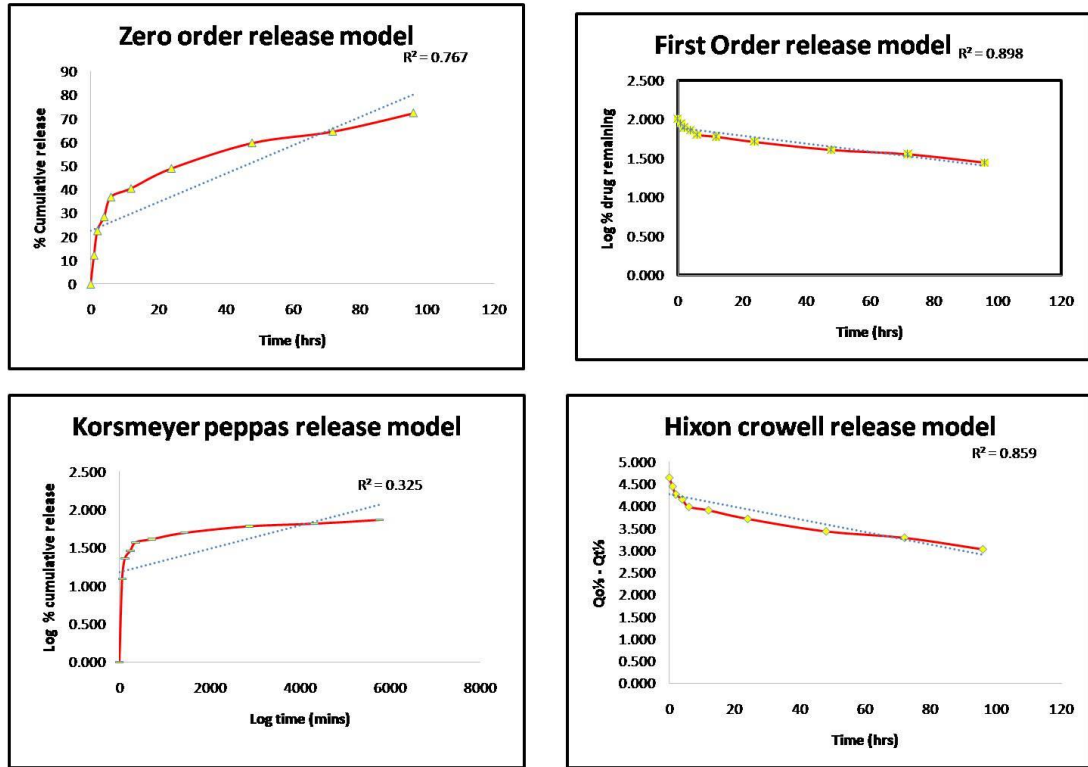


Figure 5-28 Drug release kinetic models

5.5.11 Phospholipid content by Stewart method

The calculated amount of lipids in optimized batch was 4.9 ± 0.18 mg/ml and amount of lipid found in HNCs by Stewart method was 4.36 ± 1.38 mg/ml.

5.5.12 Estimation of residual solvent by HS-Gas Chromatography

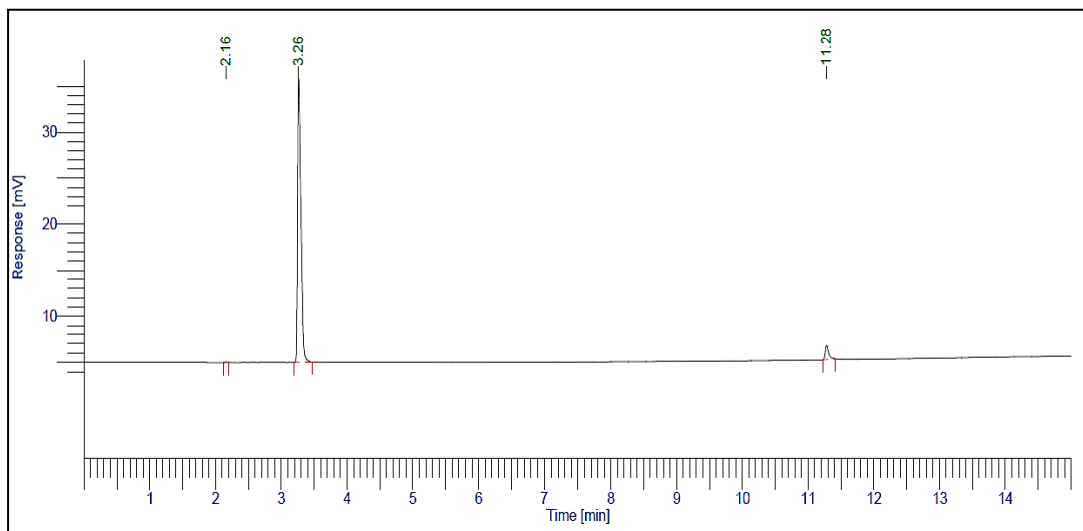


Figure 5-29 HS-GC graph for standard chloroform

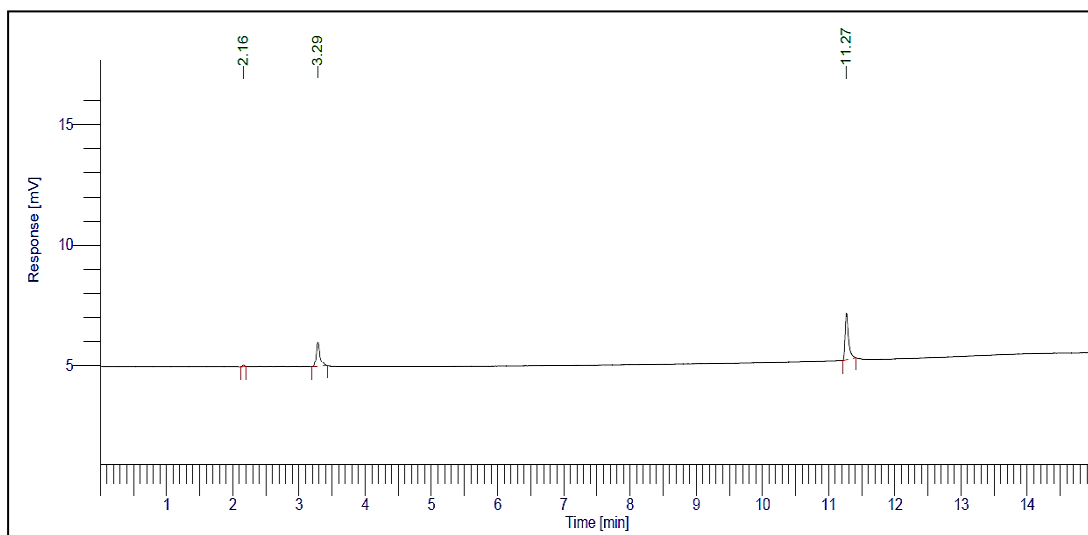


Figure 5-30 HS-GC graph for Residual solvent (Chloroform) present in HNCs formulation

Table 5-20 Residual solvent (Chloroform) Analysis

Sr No.	Standard chloroform(ppm)	Chloroform in formulation (ppm)
1	1000	32.1

The USP guidelines suggest that Chloroform is CLASS II solvent and the limit for PDE (Permitted Daily Exposure) is 0.6 mg/day equivalent to 60 ppm. From the data of the residual solvent, it was confirmed that chloroform present in the final optimized batch of HNCs is within the limits as per USP guidelines for residual solvents.

5.5.13 Small angle X Ray scattering (SAXS)

HNCs shape and architecture in three dimensions were analyzed through SAXS. Results of experimental data are given in Figure 5-31 and data are transformed into an inter-atomic vector distribution profile (Figure 5-32) which revealed 142 nm of maximum dimension and 71 nm of radius of gyration thus confirming spherical shape (Figure 5-33) of HNCs. Variation of scattering curve intensity indicates the complexity of internal structure of nanocarrier system. Intersection of all scattering curves at one point is defined as iso-scattering point relating to the external radius of the particle inaccessible to solvent. In above graph, iso-scattering point is located at $q=0.213 \text{ nm}^{-1}$ which corresponds to radius of 71 nm and diameter of 142 nm.

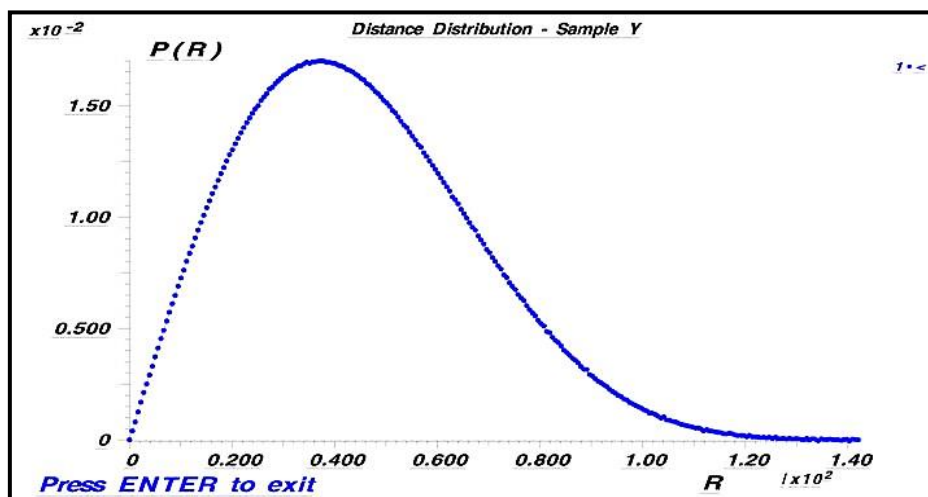


Figure 5-31 SAXS distance distribution profile

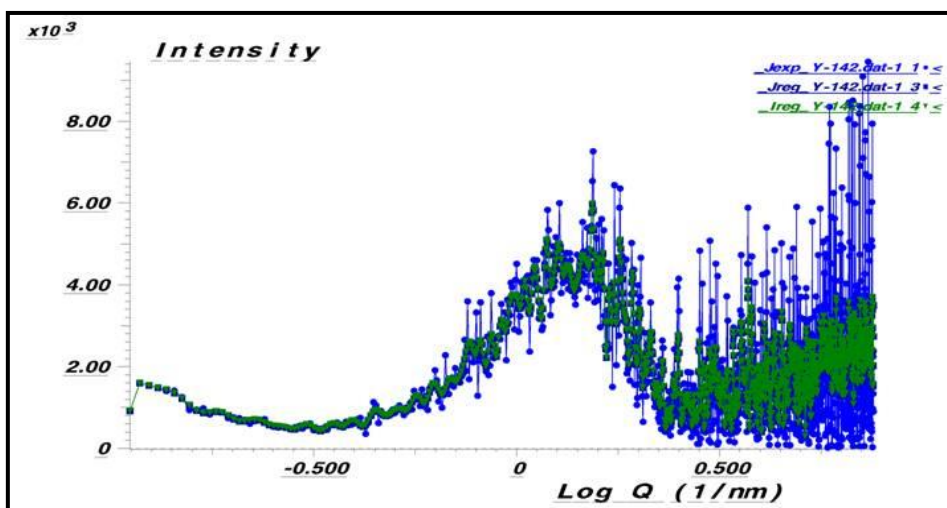


Figure 5-32 SAXS inter atomic vector distribution profile

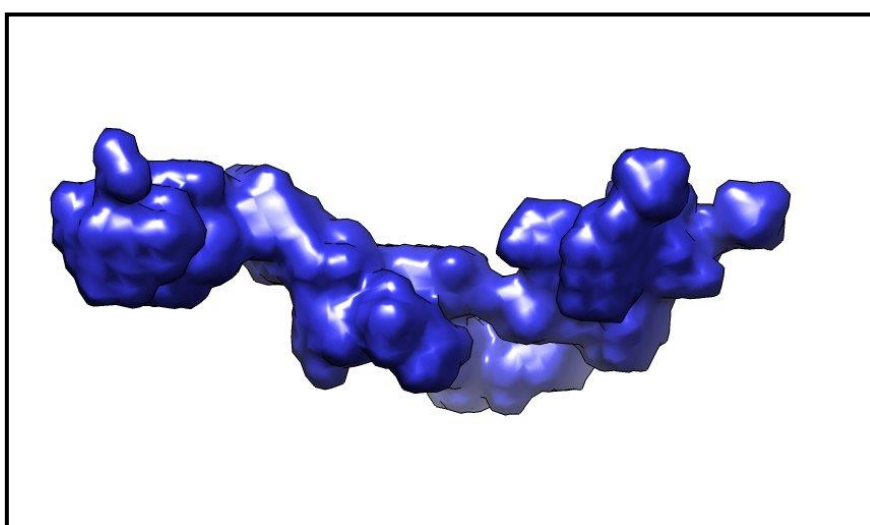


Figure 5-33 SAXS 3D modelling

5.6 REFERENCES

1. Zhang L, Zhang L. Lipid-polymer hybrid nanoparticles: synthesis, characterization and applications. *Nano Life*. 2010;1(01n02):163-73.
2. Seyednejad H, Ghassemi AH, van Nostrum CF, Vermonden T, Hennink WE. Functional aliphatic polyesters for biomedical and pharmaceutical applications. *Journal of Controlled release*. 2011;152(1):168-76.
3. Gao H, Schwarz J, Weisspapier M. Hybrid lipid-polymer nanoparticulate delivery composition. Google Patents; 2008.
4. Wasungu L, Hoekstra D. Cationic lipids, lipoplexes and intracellular delivery of genes. *Journal of Controlled Release*. 2006;116(2):255-64.

5. Chan JM, Zhang L, Yuet KP, Liao G, Rhee J-W, Langer R, et al. PLGA–lecithin–PEG core–shell nanoparticles for controlled drug delivery. *Biomaterials*. 2009;30(8):1627-34.
6. Thevenot J, Troutier A-L, David L, Delair T, Ladavière C. Steric stabilization of lipid/polymer particle assemblies by poly (ethylene glycol)-lipids. *Biomacromolecules*. 2007;8(11):3651-60.
7. Troutier A-L, Véron L, Delair T, Pichot C, Ladavière C. New insights into self-organization of a model lipid mixture and quantification of its adsorption on spherical polymer particles. *Langmuir*. 2005;21(22):9901-10.
8. Troutier A-L, Delair T, Pichot C, Ladavière C. Physicochemical and interfacial investigation of lipid/polymer particle assemblies. *Langmuir*. 2005;21(4):1305-13.
9. Stavropoulos K. *Synthesis and Characterization of Lipid-Polymer Hybrid Nanoparticles for Combinatorial Drug Delivery*: University of Kansas; 2011.
10. Zhao P, Wang H, Yu M, Liao Z, Wang X, Zhang F, et al. Paclitaxel loaded folic acid targeted nanoparticles of mixed lipid-shell and polymer-core: in vitro and in vivo evaluation. *European journal of pharmaceutics and biopharmaceutics*. 2012;81(2):248-56.
11. Liu Y, Pan J, Feng S-S. Nanoparticles of lipid monolayer shell and biodegradable polymer core for controlled release of paclitaxel: effects of surfactants on particles size, characteristics and in vitro performance. *International journal of pharmaceutics*. 2010;395(1-2):243-50.
12. Hadinoto K, Sundaresan A, Cheow WS. Lipid–polymer hybrid nanoparticles as a new generation therapeutic delivery platform: a review. *European journal of pharmaceutics and biopharmaceutics*. 2013;85(3):427-43.
13. Valencia PM, Basto PA, Zhang L, Rhee M, Langer R, Farokhzad OC, et al. Single-step assembly of homogenous lipid– polymeric and lipid– quantum dot nanoparticles enabled by microfluidic rapid mixing. *ACS nano*. 2010;4(3):1671-9.
14. Thevenot J, Troutier A-L, Putaux J-L, Delair T, Ladavière C. Effect of the polymer nature on the structural organization of lipid/polymer particle assemblies. *The Journal of Physical Chemistry B*. 2008;112(44):13812-22.

HNCs formulation

15. Mandal B, Bhattacharjee H, Mittal N, Sah H, Balabathula P, Thoma LA, et al. Core-shell-type lipid-polymer hybrid nanoparticles as a drug delivery platform. *Nanomedicine: Nanotechnology, Biology and Medicine*. 2013;9(4):474-91.
16. USP 40 Chemical Tests, residual solvents.